Progress in Oceanography 218 (2023) 103122

Contents lists available at ScienceDirect

Progress in Oceanography

journal homepage: www.elsevier.com/locate/pocean

Transport and distributions of naturally and anthropogenically sourced trace metals and arsenic in submarine canyons

Marta Tarrés [a], Marc Cerdà-Domènech [a], Rut Pedrosa-Pàmies [a,b], Andrea Baza-Varas [a], Antoni Calafat [a], Anna Sanchez-Vidal [a], Miquel Canals [a,c,d,*]

[a] GRC Geociències Marines, Dept. Dinàmica de la Terra i de l'Oceà, Facultat de Ciències de la Terra, Universitat de Barcelona, 08028 Barcelona, Spain
[b] The Ecosystems Center, Marine Biological Laboratory, Woods Hole, MA, USA
[c] Reial Acadèmia de Ciències i Arts de Barcelona (RACAB), La Rambla 115, 08002 Barcelona, Spain
[d] Institut d'Estudis Catalans (IEC), Secció de Ciències i Tecnologia, carrer del Carme 47, 08001 Barcelona, Spain

ARTICLE INFO

Keywords:
Submarine canyons
Trace metals
Chemical pollutants
Settling particles
Seafloor sediments
SW Mediterranean Sea

ABSTRACT

Continental margins play a key role in the cycling of natural and anthropogenic trace metals (TMs) as pathways at the interface between landmasses and deep ocean basins but also as sinks. Knowledge of how short-lived forcings alter the export dynamics of TMs is essential for our understanding of their fate in that setting. Here we report time series of particulate metal fluxes in three submarine canyons —namely Escombreras, Almeria and the Garrucha-Almanzora system— of the South-Western Mediterranean Sea. Our research focuses on combining multi-elemental TMs (Al, Fe, Ti, Co, Cu, Mn, Ni, Pb and Zn) and As (a metalloid) contents of settling particles collected near the bottom by automated particle traps during one year, and seafloor sediment samples from below the traps. We assess the role of storms and bottom trawling in the off-shelf transport of particulate TMs and As, and the natural and anthropogenic contributions of TMs by using enrichment factors (EFs).

The TM export fluxes and composition changed over the study period, from March 2015 to March 2016. TM fluxes increase in early spring 2015 in association with short-lived storm events and during calm months in the Garrucha-Almanzora Canyon system, likely due to sediment resuspension triggered by bottom trawling. In terms of composition, TMs in the sinking fluxes appear to be closely associated with lithogenic (Al, Fe and Ti) and authigenic (Mn) particles' proxies. During storm events, the mass of settling particles in Escombreras and Almeria canyons was impoverished in Al, Fe, As, Co, Cu, Mn and Ni compared to other periods. The Garrucha-Almanzora Canyon system behaves differently as the above-described differences, are not observed there. Moreover, the TM composition of the sediments —with higher contents of Fe, Ti and several other TMs— in this canyon is barely tied to the composition of the settling particles. Finally, Cu and Zn contents, together with Pb in the northernmost Escombreras Canyon, are best explained by referring to anthropogenic sources. This work provides insights into the profound influence of the natural and anthropogenic forcings controlling the distributions and seasonal dynamics of particulate TMs and As in submarine canyons.

1. Introduction

Trace metals (Al, Fe, Ti, Co, Cu, Mn, Ni, Pb, and Zn; TMs hereafter) in the marine environment have attracted the interest of researchers due to their critical role in regulating the growth and structure of marine organisms, and their interest as tracers of oceanographic processes, and also as pollutants (Morel and Price, 2003, Twining and Baines, 2013; Jeandel and Vance, 2018). Suspended particles are known by their capability to remove TMs from seawater (Anderson and Hayes, 2015 and references therein). Biological uptake, scavenging onto particle surfaces and precipitation (including bacteria-mediated) incorporate TMs into the particulate phase within the water column (Cowen and Bruland, 1985; Morel and Price, 2003; Anderson, 2020). The cycling of metals is, therefore, driven by sedimentary dynamics controlling the input, production, transformation, transport and accumulation of particles along the water column down to the seafloor. In other words, the distribution of TMs in the ocean is largely regulated by sinking particle fluxes (Huang and Conte, 2009; Kuss et al., 2010; Theodosi et al., 2013; Conte et al.,

* Corresponding author.
E-mail address: miquelcanals@ub.edu (M. Canals).

https://doi.org/10.1016/j.pocean.2023.103122
Received 26 April 2023; Received in revised form 1 September 2023; Accepted 5 September 2023
Available online 9 September 2023

2019). Within the fluxes, the lithogenic, authigenic (abiotically precipitated) and biogenic fractions are vectors of TMs and As towards the seafloor (Huang and Conte, 2009). In the last years, researchers have employed some individual elements as proxies for mineral phases (e.g., Ba, Fe or Mn for authigenic minerals; Al, Fe or Ti for lithogenic minerals; and P for biogenic minerals, among others) (Sanchez-Vidal et al., 2005; Twining and Baines, 2013; Ohnemus and Lam, 2015; Al-Hashem et al., 2022). Those proxies provide information on transfer vectors and processes involving all other TMs, as elements associated with the same type of particles often exhibit similar distributions (Lee et al., 2018).

Continental margin settings are known as major vectors and suppliers of particulate and dissolved TMs to the deep basins (Lam et al., 2006; Charette et al., 2016; Lemaitre et al., 2020), and also as TMs' sinks (Palanques et al., 2008; Anderson, 2020). Particle transport in continental margins is driven by currents, which eventually can also erode and re-suspend seafloor sediments that will then add to the pool of particles in the water column (Heussner et al., 2006). Ultimately, such particles will be buried with their TMs' load (Geibert, 2018). TM cycling results from a complex interplay of physical and biogeochemical processes and is therefore difficult to understand (Noble et al., 2012). This is well illustrated by high-energy events such as sea storms or dense shelf water cascades (DSWC), which intensify TMs' transport from shallow to deep environments while also enhancing biogeochemical interactions (Hung and Ho, 2014; Dumas et al., 2014; Cossa et al., 2014; Durrieu de Madron et al., 2023). However, beyond the widely recognized key role of continental margins in mediating TMs' transport to the open ocean, significant gaps persist about the distribution of particulate metals and the processes determining their seaward transport, including deep continental margin regions (Palanques et al., 2008; Jesus et al., 2010; Roussiez et al., 2012; Cossa et al., 2014).

Besides, there is clear evidence that anthropogenic TMs have added to natural fluxes along and across continental margin settings and beyond, especially since the mid-nineteenth century (Grousset et al., 1995; Hanebuth et al., 2018), thus contributing to the degradation of the environmental status of our coasts, seas and oceans (Papale et al., 2018; Azaroff et al., 2020). In some places such inputs have been traced back to the Roman Period (Mil-Homens et al., 2016).

This study addresses some of these unknowns in three submarine canyons located off southeast Spain in the Mediterranean Sea (cf. section 2.1). These canyons connect coastal and shelf environments to the deep-sea (Ross et al., 2009; Puig et al., 2014). This paper is a follow up of a previous one by Tarrés et al. (2022) focusing on the major components of settling particles in the investigated submarine canyons for the same period. In the present paper, we focus on the multi-elemental TM (Al, Fe, Ti, Cu, Co, Mn, Ni, Pb, and Zn) and As (a metalloid) contents in settling particles and assess the processes controlling the dynamics of TMs and As in submarine canyons. By comparing the seafloor sediment composition with particles sinking in the canyons we provide insights into the processes leading TMs to reach canyon floors and their preservation in the sedimentary record. Finally, the calculation of enrichment factors (EFs) allows for estimating the anthropogenic influence on TM fluxes.

For the purpose of this paper and for ease of simplicity, from here onwards we will refer to all elements listed above including As as TMs, i.e. those which appear in the relevant environmental matrix with ppm or ppb concentrations. This will include Al and Fe, which according to their concentrations actually appear as TMs in particle fluxes in the water column though not in the analyzed sediments, where they display concentrations of thousands of ppm.

2. Study area

2.1. Overall setting

The study area encompasses three margin segments in the SW Mediterranean Sea, namely Mazarron and Palomares, located on the western edge of the Algero-Balearic Sea, and the Almeria one, located on the northeastern border of the Alboran Sea (Fig. 1a, b). The continental shelf is narrow (<13 km) (Lobo et al., 2014), with the shelf edge located between 100 and 200 m depth. It is cut by several submarine canyons of small to medium size (Pérez-Hernández et al., 2014), which are smaller and more densely grouped to the north (Acosta et al., 2013). The three submarine canyons here investigated are, from north to south, Escombreras Canyon, Garrucha-Almanzora Canyon system and Almeria Canyon.

Surface circulation is influenced by the Northern Current flowing southward in the Gulf of Vera (Fig. 1b) and the entry of Atlantic Water into the Alboran Sea (e.g. Vargas-Yáñez et al., 2002; Macias et al., 2016). The latter forms two gyres known as the Western Alboran Gyre (WAG) and the Eastern Alboran Gyre (EAG). The two flows converge at the Almeria-Oran Front (AOF) from where surface waters are redirected towards the Algerian continental margin (Tintore et al., 1988) (Fig. 1b). Intermediate and deep waters flow westwards towards the Strait of Gibraltar (Parrilla et al., 1986; Millot, 1999).

Rivers opening into the study area are dry most of the year due to the semi-arid regional climate. However, short-lived flood events may supply substantial volumes of water, sediment (and also litter) to the coastline. The main rivers in the study area are the Almanzora and Andarax, which discharge in the Gulf of Vera and the Gulf of Almeria, respectively (Fig. 1b). Off-shelf transfer of sedimentary particles is driven by storm events triggering high waves and increasing currents velocities over the continental shelf, subsequently resulting in the resuspension of shelf floor sediments (Lobo et al., 2014). Several such stormy periods during the sampling period in this study have been previously documented (Supplementary Fig. 1; see further details in Tarrés et al., 2022). Several wet NE storms occurred at the beginning of the study period, i.e. in late March and early April 2015. Storms in the following months were of limited intensity and range. The situation changed in autumn months, when several rainfall episodes led to a noticeable increase in the discharge of Almanzora and Andarax rivers, with the main event in early November 2015. Finally, several SW dry storms took place by the end of the year-round study period.

Sediment transfer into the Garrucha-Almanzora Canyon system is favoured by the overall geomorphic configuration of the margin, with a canyon-incised narrow continental shelf, and the closeness of canyon heads to the mouths of Almanzora River but also Antas and Aguas rivers (Fig. 1b) (Puig et al., 2017). Enhanced fluxes recorded during summer months in this canyon system have been attributed to bottom trawling activities in the area (Tarrés et al., 2022).

2.2. Total mass fluxes

Total mass fluxes (TMF) in the three investigated canyons, including the elemental composition and grain sizes of the particles involved, were described in a previous publication (Tarrés et al., 2022 and references therein). A summary is provided here as background information, including topic specific interpretations wherever judged convenient.

A common feature is that in all three canyons mass fluxes were predominantly composed of lithogenic particles, accounting for approximately 61%, 62%, and 72% in Escombrereras, Garrucha-Almanzora, and Almeria canyons, respectively. The carbonate fraction constituted the second-largest in the fluxes, representing about 37%, 34%, and 24% in the above canyons, respectively. The difference in $CaCO_3$ contents between the two canyons in the Gulf of Vera and Almeria Canyon, further south, was partially attributed to inputs of detrital material containing $CaCO_3$. OM was a small fraction, representing only 3–4% of the TMF in those canyons. The clay and silt fractions dominated the fluxes in all three canyons, with small standard deviations < 4%. This suggested a consistent sorting of the material being transported in suspension towards the distal margin.

Regarding flux magnitudes, Escombreras Canyon —measured from March to August 2015— exhibited two distinct situations. At the beginning of the study period, the trap collected comparatively high

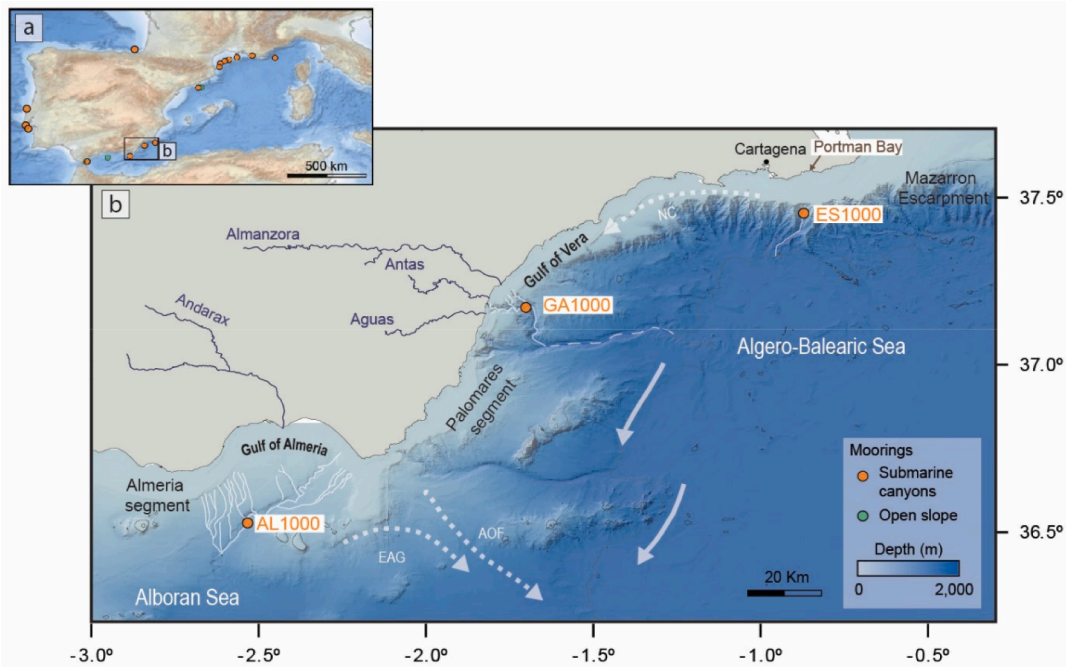

Fig. 1. (a) Map of the Western Mediterranean Sea and nearby areas showing places where trace metal contents and fluxes have been measured according to the literature and also from this study (cf. section 4 and Fig. 6). Map after EMODnet (https://emodnet.ec.europa.eu/geoviewer). (b) Shaded relief bathymetry map off SE Spain displaying the location of the mooring lines within the Escombreras Canyon (ES1000), the Garrucha-Almanzora Canyon system (GA1000) and the Almeria Canyon (AL1000). White lines indicate canyon axes including tributaries if present. Discontinuous white line indicate Alias-Almanzora Canyon axis, when the Garrucha-Almanzora system merges with the southern system. The general surface circulation (discontinuous white arrows) and the intermediate and deep circulation are outlined (continuous white arrows). Main rivers are also shown (blue lines). AOF: Almeria-Oran Front. EAG: Eastern Alboran Gyre. NC: Northern Current. (For interpretation of the references to color in this figure legend, the reader is referred to the web version of this article.)

fluxes during storm events in March and April 2015 (Fig. 2a). Within this time, strong currents led to the resuspension and export of particulate matter from the continental shelf into the neighboring canyons, eased by nepheloid layers. The $CaCO_3$ content increased in March 2015 due to particle resuspension and advection of previously settled biogenic $CaCO_3$ from the shelf. In contrast, minimal fluxes were collected from late April to August, corresponding to calm meteorological and oceanographic conditions.

Mass fluxes in the Garrucha-Almanzora Canyon system —measured from March to September 2015— also peaked during the March and April 2015 storms (Fig. 2a). In this canyon system, bottom trawling activities around the canyon generated a nepheloid layer at depths exceeding 400 m, subsequently promoting increased particle fluxes throughout the spring and summer months (Fig. 2a). The incision of canyon heads into the continental shelf and the short distance of their heads to river mouths facilitated the transfer of terrestrial organic matter (OM, about 5% of the TMF) during the stormy spring period. Conversely, $CaCO_3$ contents displayed higher values during the summer months, correlating with TMFs. Therefore, such higher contents were not due to lesser dilution within the lithogenic fraction. In terms of particle sizes, there was a coarsening effect after May, with relatively high sand contents (up to 4.5%) for the lithogenic particles, especially in May, late August and September 2015.

Particle fluxes in Almeria Canyon —measured from March 2015 to March 2016— remained consistently low throughout the entire period. Similarly to the other two canyons, higher downward fluxes were observed at the beginning of the study period (Fig. 2a), coinciding with spring storm events. Mass fluxes showed a slight increase between November 2015 and January 2016, likely due to short-lived storms and several rainfall episodes that increased water discharge from nearby rivers, especially in early November. By the end of the monitoring period in February-March 2016, dry western storms occurred, which did not enhance downward fluxes at the trap location (Fig. 2a). In terms of composition, $CaCO_3$ contents increased during the spring 2015 and winter 2016 storm events, likely due to lateral transport, as previously explained for the Escombreras Canyon. OM presented a more pronounced seasonal pattern, with a higher contribution (about 7%) to mass fluxes during summer months, which can be explained by overall lower mass fluxes. In late January, OM contents increased again to about 6% due to the arrival of biogenic material from surface primary production. In terms of particle sizes, coarser fractions were collected at the beginning of the study period, with the higher sand content (about 6%) coinciding with the March storm. No coarsening trend in the fluxes was noticed during subsequent storms.

3. Materials and methods

3.1. Sampling

Sea work was performed during research cruises NUREIEV-1 from 13 to 24 of March 2015, NUREIEV-2 from August 29 to September 5, 2015, and NUREIEV-3 from 23 to 30 of April 2016, onboard R/V Ángeles Alvariño.

Three mooring lines —named ES1000, GA1000 and AL1000, respectively— were deployed along the axis of the Escombreras Canyon, the Garrucha-Almanzora Canyon system and the Almeria Canyon at 985, 1,100 and 1,000 m depth, respectively, from March 2015 to March 2016 (Fig. 1b and Supplementary Table 1; cf. section 2.1). Each mooring was equipped with a Technicap PPS3/3 sequential particle trap (aperture 0.125 m^2, cylindroconical shape) with 12 cups at 25 m above the bottom and a sampling interval of 7–16 days. Acid cleaned trap cups were filled with 5% (v/v) formaldehyde solution in 0.45 μm filtered sea water buffered with sodium tetraborate. Within the entire sampling period, only 10 days were devoted to mooring recovery, maintenance and redeployment operations during which there was no sample collection. Failures in the particle trap rotating system of ES1000 and GA1000

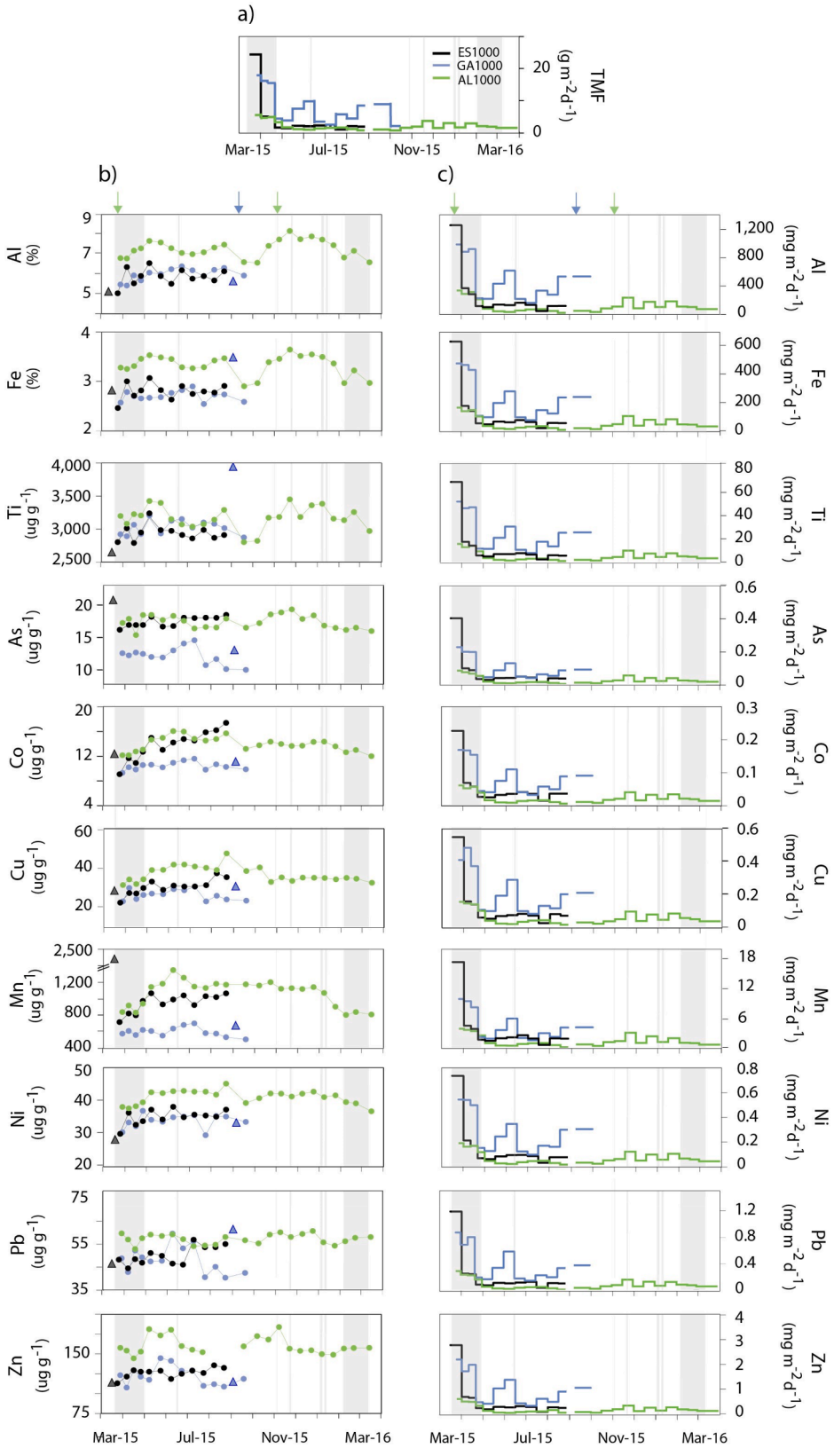

Fig. 2. Time series of (a) Total mass fluxes in settling particles at stations ES1000 (black line), GA1000 (blue line) and AL1000 (green line) after Tarrés et al. (2022). (b) Trace metal contents —in μg g^{-1} excepting Fe and Al, which are in %— in settling particles (dots) and seafloor sediments (triangles) at stations ES1000 (black dots), GA1000 (blue dots) and AL1000 (green dots). (c) Trace metal fluxes in settling particles. Color codes as in (a). Black and blue triangles indicate trace metal and As contents in seafloor sediments from ES1000 and GA1000, respectively. Grey vertical stripes highlight sea storm events, with two main periods at the beginning and at the end of the study period (cf. Supplementary Fig. 1 for further details). The arrows above (b) and (c) plots mark river discharge events (green when close to AL1000 and blue when close to GA1000). Note that vertical scales change from one plot to the other. (For interpretation of the references to color in this figure legend, the reader is referred to the web version of this article.)

stations prevented the collection of samples during the last seven and six months, respectively.

Seabed sediment was collected with a KD Denmark multicorer at 1,002 m depth in the Escombreras Canyon during research cruise NUREIEV-1 in March 2015, and at 1,142 m depth in the Garrucha-Almanzora Canyon system during cruise NUREIEV-2 in September 2015. The sediment cores were subsampled onboard. The cores were sliced every 0.5 cm from the core top down to 5 cm, and every 1 cm from 5 cm to the core bottom. The subsamples thus obtained were stored at 2–4 °C in plastic bags. We used the top 0.5 cm of the cores for our

analyses.

3.2. Sample analysis

The seafloor sediments were freeze-dried and homogenized for later analysis. Trap samples were also freeze-dried after removing the swimmers (i.e., those organisms deemed to have entered alive the traps, Pagès et al., 2007) using a nylon mesh of 1 mm and hand-picking the smallest ones. A high precision peristaltic pump allowed obtaining a working aliquot of each sample, which was then centrifuged with ultrapure water (Milli-Q) to extract the salt and the formaldehyde solution from the trap's cups. Trap sample processing is described in detail in Rumín-Caparrós et al. (2016).

The elemental composition was determined using a Perkin-Elmer Elan-6000 ICP-MS and a Perkin Elmer Optima 8300 ICP-OES at *Centres Científics i Tecnològics de la Universitat de Barcelona* (CCiT-UB). A two-step extraction method was applied for sample digestion. The first step was carried out in a closed digestion system with the goal of avoiding the loss of volatile elements, such as As. The leached elements were then recovered before proceeding with the second step, under open system conditions. The samples were placed in a Teflon reactor closed digestion system with 2.5 mL of HNO_3 (65%) during at least 12 h in a stove at 90 °C. The extract was centrifuged to collect the supernatant and obtain a first solution, thus recovering the leached elements. The solid sample recovered from centrifugation was placed again into a Teflon reactor, and digested with 2.5 mL (65%) HNO_3, 10 mL (40%) HF and 2 mL (70%) $HClO_4$ during at least 12 h in a stove at 90 °C. Then, the Teflon reactor was heated in a sand bath at 250 °C. 2 mL of (65%) HNO_3 and 2 mL of H_2O_2 were added and heated again until total evaporation of the acid volume. When the sample showed incipient dryness, 2 mL $HClO_4$ were added until reaching the total evaporation of the acid. The residue was redissolved in 2 mL HNO_3 and 5 mL of ultrapure water (Milli-Q) to obtain a second solution. Two procedural blanks were analyzed with each sample batch to ensure the lack of contamination during sample processing and analysis. Replicates were routinely performed to determine the uncertainty associated to subsampling heterogeneity and method precision. Relative standard deviation (RSD) was always below 5% for all metals, except for Pb and Ni (~6.5%) and Mn (7.5%). For As, the RSD was 5.4%.

3.3. Data analysis

Particulate fluxes in the investigated canyons have been previously published in Tarrés et al. (2022) for the same period of time here addressed. Those fluxes allow calculating the annual Time Weighted Fluxes (TWF) of TMs, which represent a weighted average of TMFs corrected according to the number of sampling days:

$$TWF\left(mgm^{-2}d^{-1}\right) = \frac{\sum Mi(mg)}{Collectionarea(m^2)^* \sum Di(d)} \quad (1)$$

where M_i is the mass per sample and D_i is the total days of collection.

The annual Time Weighted Content (TWC) is calculated for each element to correct sampling interval values, following equation:

$$TWC\left(\mu g g^{-2}\right) = \frac{TWF(elementmass)}{TWF(totalmass)} \quad (2)$$

The correlations between variables, including major and trace elements, is evaluated by means of the Pearson's Correlation Coefficient (PCC) for each station, considering $p < 0.05$ as significant.

A Principal Component Analysis (PCA) allowed identifying the dominant factors describing the variability of the dataset. PCA variables are the same than for PCC, including OM and $CaCO_3$ main flux components from Tarrés et al. (2022). Lithogenic components were represented by Al, Fe and Ti contents. However, to simplify the dataset, Ti from GA1000 was excluded from the analysis. Biogenic silica was not included given its very minor contribution to the fluxes (Tarrés et al., 2022). AL-I-11 and AL-I-12 samples from AL1000 station were also excluded due to Zn outliers. The dataset was standardized in order to adjust the variance of all variables to the same scale. Data standardization consisted in subtracting the mean of all variables and dividing each one by its standard deviation. It was also conducted on log-transformed contents to improve the normal distribution of the variables (Karageorgis et al., 2009). A Varimax rotation subroutine was performed after the PCA to facilitate the interpretation of the flux components. All statistical analyses have been carried out using the *Statgraphics Centurion* software.

To explore potential statistical differences in TM contents between stations (ES1000, GA1000, and AL1000) and periods within each station (stormy vs. calm periods), we used the Kruskal-Wallis H non-parametric test since normality was not achieved when considering the full dataset. TMs pollution levels are calculated using EFs, which are usually applied to estimate anthropogenic contributions to marine sediments (Birch, 2017). This method requires normalizing metal values to reduce content's variability resulting from natural changes in mineralogy and grain size (Aloupi and Angelidis, 2001; Roussiez et al., 2006). Given the rather diverse particle composition of trap samples, partly due to variations in rock composition inland, a normalization step was applied to compensate for such natural variations. We used Al as the normalizing element as in previous studies (Palanques et al., 2008; Mil-Homens et al., 2013a; Dumas et al., 2014). Pre-industrial background ratios have been estimated from subseafloor sediments in the Almeria and Escombreras canyons, as obtained from ^{210}Pb dating of sediment subsamples at relevant core depths (50–51 cm) from the same location of the Escombreras Canyon sediment trap (unpublished data), which have been extended to the Almeria Canyon (40–41 cm). Whereas in the Garrucha-Almanzora Canyon system this has not been possible since the corresponding multicore reached 15 cm below the seabed only. Therefore, the samples collected in the GA1000 trap were normalized with the subseafloor sediments of the Almeria Canyon given the strong similarity in the mineralogical composition of clay minerals from both canyons. EFs were obtained following equation [3] while also considering a threshold of 1.5 as indicative of anthropogenic contributions according to local pre-industrial values (Roussiez et al., 2006):

$$EF = \frac{TM/Al}{TM_b/Al_b} \quad (3)$$

where TM and Al refer to TM and Al contents in the sample, respectively, and TM_b and Al_b represent the pre-industrial levels.

4. Results

4.1. Trace metal contents in settling particles and fluxes

TM contents in settling particles change from one station to the other (Table 1 and Fig. 2b). The highest contents correspond to AL1000 station for all elements, as illustrated by As and Al with 19.36 μg g^{-1} and 8.19% peak values, respectively. One exception is the Co, which increases at ES1000 station with 17.42 μg g^{-1}. Minimum values for As, Mn, Ni, Pb and Zn occur at station GA1000, while the lowest ones for Al, Fe, Ti, Cu, and Co appear at ES1000 (Table 1).

The highest differences between minimum and maximum TM values occur at AL1000 station, with a remarkable difference for the Mn (from 791.07 to 1,347.46 μg g^{-1}) and the Ti (from 2,790.89 to 3,454.70 μg g^{-1}) relative to the other two stations. However, Co displays the highest variability at ES1000 (from 9.09 to 17.42 μg g^{-1}), while Pb and As do it at GA1000 (from 40.27 to 59.49 μg g^{-1} and from 9.97 to 14.53 μg g^{-1}, respectively) (Table 1). Fig. 2b shows how TM contents changed during one year (AL1000 station) or half a year (ES1000 and GA1000). In AL1000, some elements reach their highest contents in spring-summer (e.g. Co, Cu, Mn), while others do in late spring-summer and autumn (e.g. Al, Fe, Ti, As, Ni, and Zn). Pb values are rather steady and do not

Table 1
Trace metal contents and fluxes in settling particles and seafloor sediments (SS). AL1000 values correspond to a complete annual cycle, whereas GA1000 and ES1000 values correspond to a half-year period. *: Average metal contents in time-weighted content (TWC). **: Average metal fluxes in time-weighted flux (TWF).

Code		**ES1000**			**GA1000**			**AL1000**			**SS ES1000**	**SS GA1000**
Depth (m)		985			1,100			1,000			1,002	1,142
Number of samples		12			13			24				
Content	% or μg g^{-1}	Average*	Max	Min	Average*	Max	Min	Average*	Max	Min		
Al	%	5.54	6.60	5.10	5.97	6.42	5.47	7.31	8.19	6.60	5.13	5.66
Fe	%	2.72	3.14	2.54	2.77	2.98	2.62	3.40	3.72	2.98	2.82	3.49
Ti	μg g^{-1}	2,866.65	3,185.58	2,783.64	2,991.74	3,161.40	2,858.56	3,183.20	3,454.70	2,790.89	2,649.18	3,944.93
As		16.79	18.47	16.18	11.83	14.53	9.97	17.36	19.36	15.40	20.79	13.09
Co		11.41	17.42	9.09	10.21	11.58	9.28	13.55	16.10	12.04	12.36	11.10
Cu		26.24	37.38	22.11	25.65	30.30	22.68	35.34	47.80	31.36	25.00	27.54
Mn		816.99	1,057.47	702.08	563.31	686.94	489.12	1,005.10	1,347.46	791.07	2,359.08	664.77
Ni		32.32	37.87	29.55	33.04	36.56	29.06	40.26	45.07	36.56	28.26	33.37
Pb		48.90	56.95	44.48	47.45	59.49	40.27	57.31	60.85	53.02	46.56	61.26
Zn		119.97	135.70	113.12	122.31	144.47	107.20	158.08	184.06	144.90	114.12	115.46
Flux**	mg m^{-2} d^{-1}	Average**	Max	Min	Average**	Max	Min	Average**	Max	Min		
Al		266.11	1,272.47	58.00	463.65	1,000.66	173.59	119.83	349.83	33.52	–	–
Fe		130.66	633.22	27.94	214.67	479.88	82.94	55.81	171.43	15.79	–	–
Ti		13.76	69.76	2.90	23.22	52.90	8.38	5.22	16.36	1.47	–	–
As		0.08	0.40	0.02	0.09	0.23	0.04	0.03	0.09	0.01	–	–
Co		0.05	0.23	0.02	0.08	0.17	0.03	0.02	0.06	0.01	–	–
Cu		0.13	0.55	0.03	0.20	0.49	0.08	0.06	0.16	0.02	–	–
Mn		3.92	17.52	0.99	4.37	10.17	1.91	1.65	4.23	0.52	–	–
Ni		0.16	0.74	0.03	0.26	0.54	0.10	0.07	0.19	0.02	–	–
Pb		0.23	1.20	0.05	0.37	0.88	0.16	0.09	0.31	0.03	–	–
Zn		0.58	2.82	0.12	0.95	2.23	0.36	0.27	0.81	0.11	–	–

increase at any specific season. The half year records from ES1000 show an increasing trend from March to August 2015 for Co, Cu, Mn and Zn, while Pb is higher during July and August. In the GA1000 station only Al raises throughout most of the period, while other elements diminish during the last months, as shown by As, Co, Cu, Mn, Pb and Zn. In fact, As, Co, Cu and Mn reach their higher concentrations in June. In contrast, Pb and Zn peak during late spring months. Fe correlates well with Mn ($r^2 = 0.85$; $p < 0.01$) at GA1000, whereas Fe and Ti correlate with Al at ES1000 and AL1000 ($r^2 > 0.78$; $p < 0.01$) (Supplementary Table 2).

Our time series shows several TM export events during the investigated period (Fig. 2c). A first and most noticeable flux increment, at the beginning of the sampling period, resulted in the highest measured export rates for all elements under consideration, with minimum values for Co up to 0.23, 0.17 and 0.06 mg m^{-2} d^{-1} and maximum values of 1,272.47, 1,000.66 and 349.83 mg m^{-2} d^{-1} for Al at stations ES1000, GA1000 and AL1000, respectively (Table 1 and Fig. 2c). Minor but consistent increments of all elements were recorded at GA1000 in late May, early June, late August and September 2015 (Fig. 2c), which coincided with high turbidity values from 400 m depth down to the bottom at 1,100 m (Tarrés et al., 2022). The early June 2015 peak was noticeable for its comparatively high Cu, Mn, Ni, Pb and Zn export fluxes, whereas As and Co showed values closer to the ones found during the ensuing summer events (Fig. 2c). Time series for the following months are available for AL1000 station only. A slight flux increment with maxima ranging between 0.04 and 248.52 mg m^2 d^{-1} for Co and Al, respectively, were observed between November 2015 and January 2016. TM fluxes lowered during February and March 2016 (Fig. 2c).

4.2. Trace metal contents in seafloor sediments

With few exceptions, TM contents in seafloor sediments are close or very close to the ones in settling particles (Fig. 2b). The highest contents of Ti, As, Mn and Pb (20.79, 3,944.93, 2,359.08 and 61.26 μg g^{-1}, respectively) found in this study correspond to sediments (Table 1 and Fig. 2b). At ES1000, As and Mn contents in sediments were 19% (20.79 vs. 16.79 μg g^{-1}) and 65% (2,359.08 vs. 816.99 μg g^{-1}) higher, respectively, than average contents in sinking particles (Tables 1 and 2). Sediments collected below GA1000 station show higher Fe (20.7% more), Ti (24.2% more), Mn (15.3% more) and Pb (22.5% more) contents than average contents in settling particles (Tables 1 and 2). These increments persist after normalizing TMs/Al. Furthermore, the Al-normalized values show moderate increases (<15%) for Co in ES1000, and for As, Co and Cu in GA1000 (Table 2).

4.3. Outcomes of the multivariate analysis

In the ES1000 station, four components explain 93% of the total variance of the dataset (Fig. 3a). Component 1 (53% of the total variance) is characterized by capture majority of individual variance for Co, Cu, Mn (57–77%) and to lesser extent, As, (43%). Component 2 (27% of the total variance) explains most of the variability of lithic elements (Al, Fe, Ti) (51–71%) and also of $CaCO_3$, which displays negative loading. Component 3 (8% of the total variance) is contributed by several TMs (As, Co, Cu, Pb and Zn), and explains most of the variance of Pb (56%) and Zn (85%) and, to lesser extent As (43%). Component 4 (5% of the total variance) describes most of OM variance (70%) and part of Zn variance (22%).

In the GA1000 station, four components explain 90% of the total variance of the dataset (Fig. 3b). Component 1 (49% of the total variance) describes>80% of Cu and Mn variance, and>50% of Fe, As and Co

Table 2
Trace metals and As excess (%) in canyon floor sediments with respect to time weighted contents calculated after settling particles data (both non-normalized and normalized to Al).

	Escombreras Canyon		Garrucha-Almanzora Canyon system	
		TMs/Al		TMs/Al
	%	%	%	%
Fe_{xs}	3.7	–	**20.7**	–
Ti_{xs}	−8.2	–	**24.2**	–
As_{xs}	**19.2**	**25.3**	9.6	**14.3**
Co_{xs}	−7.6	**14.6**	8.1	**12.9**
Cu_{xs}	−5.0	2.9	6.9	**11.8**
Mn_{xs}	**65.4**	–	**15.3**	–
Ni_{xs}	**−14.3**	−5.7	1.0	6.2

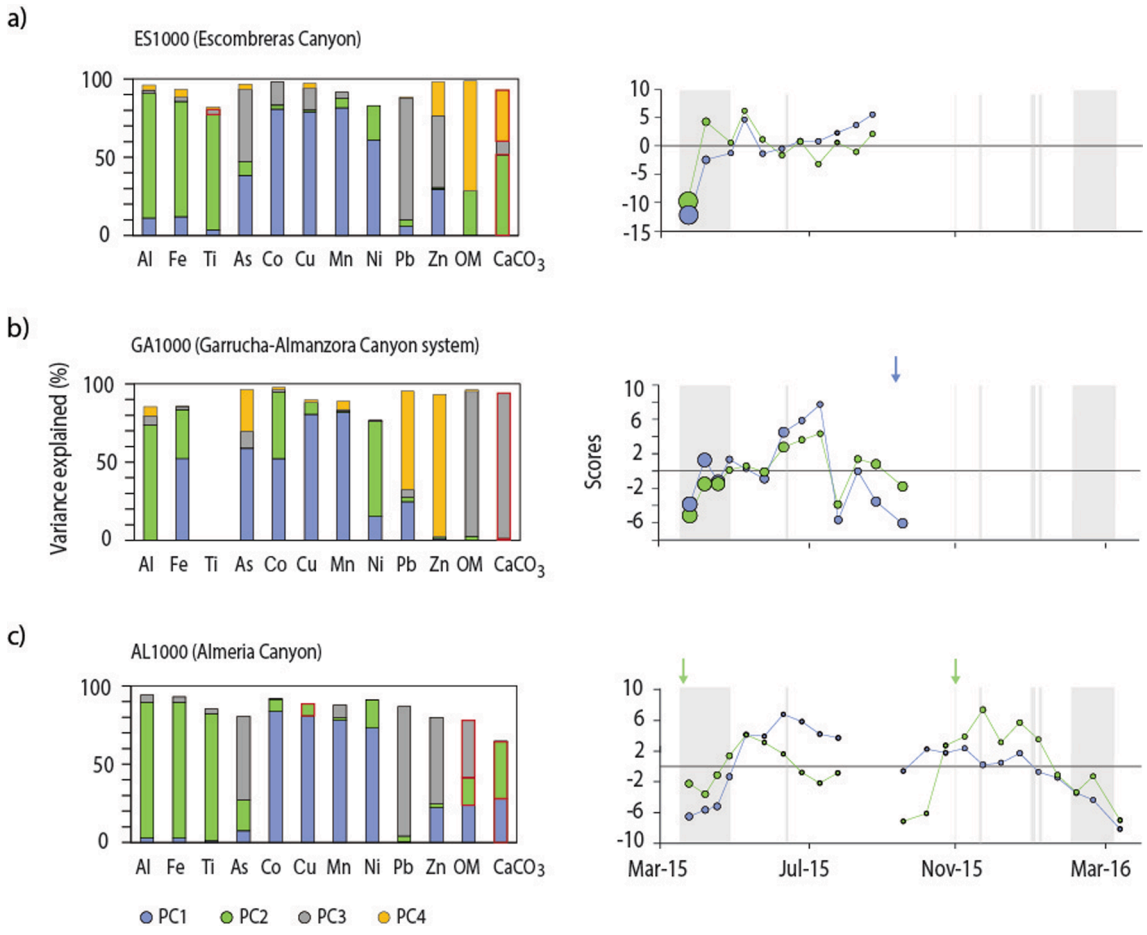

Fig. 3. Principal Component Analysis (PCA) of settling particles at (a) ES1000 (N = 11), (b) GA1000 (N = 13) and (c) AL1000 (N = 22) mooring stations. Note that some samples have been excluded from analysis due to it including outliers in the dataset. The plots explain de variance (%) for trace metals, organic matter (OM) and $CaCO_3$ after the main components (negative loads are highlighted in red in the corresponding bars of the left side plots), and the temporal variability of the scores for the two principals components (right side plots). Dot size is proportional to mass flux. (For interpretation of the references to color in this figure legend, the reader is referred to the web version of this article.)

variance. Component 2 (21% of the total variance) describes Al variance (>70%), Fe (31%), Co (42%) and Ni (61%). Component 3 (12% of the total variance) is contributed (>90%) by OM and $CaCO_3$ (negative loadings). Component 4 (8% of the total variance) explains most of Zn variance (91%) and, to a lesser extent, Pb (63%) and As (26%).

In the AL1000 station, three components explain 85% of the total variance of the dataset (Fig. 3c). Component 1 (46% of the total variance) reflects most of Co, Cu, Mn and Ni variance (>75%) and to a lesser extent Zn (29%) and OM (24%), with negative loading of $CaCO_3$ (28% of variance). Component 2 (25% of the total variance) greatly explains the variance of Al, Fe, Ti (>80%). As and Ni are also associated to the elements that represent lithogenic minerals, explaining about 20% of their individual variability). This component also captured part of $CaCO_3$ variance (35%), contributing with a negative loading. Component 3 (14%) relates most of Pb (83%) and As and Zn (~55%) variance.

5. Discussion

5.1. Intraannual variability of trace metal fluxes

TM export rates in the investigated submarine canyons are comparable to those found in former studies of submarine canyons and open slopes of the Western Mediterranean Basin (Puig et al., 1999; El Khatab, 2006; Heimbürger et al., 2012; Cossa et al., 2014). During the monitored period, the main TM export event into the studied canyons occurred in early spring 2015, concurrently with eastern storms with significant wave heights (Hs) above 4 m (cf. section 2, Fig. 2 and Supplementary Fig. 1). During the following calm months, our traps recorded several TMs pulses in the Garrucha-Almanzora Canyon system (Fig. 2c), which we attribute to bottom trawling activities on the canyon flanks, as there is no other plausible explanation. A number of studies has shown trawling activities to cause seafloor erosion and sediment resuspension (Martín et al., 2007; Puig et al., 2012; Martín et al., 2014), subsequently modifying the behavior and the biogeochemistry of OM, TMs and other pollutants in the marine environment (Bradshaw et al., 2012; Pusceddu et al., 2014; Paradis et al., 2021; Palanques et al., 2022). After October 2015, only the AL1000 station in the Almeria Canyon remained operational. Slightly higher export fluxes were recorded there between November 2015 and January 2016 after short-lived storms and rainfall episodes, mainly in early November. In short, storms and bottom trawling appear as the main triggers of TM transport events into the investigated submarine canyons.

5.2. Intraannual variability of trace metal contents in settling particles

Settling particles are vectors for TM export, which are known to be associated with lithogenic, biogenic and authigenic carriers (Huang and Conte, 2009; Conte et al., 2019; Blain et al., 2022). Specific TMs have been used as proxies of particle types, such as Fe, Al and Ti for the lithogenic fraction (Ohnemus and Lam, 2015; Lee et al., 2018), or Fe and Mn for the authigenic fraction (Martín et al., 1983; Cowen and Bruland, 1985; Bruland and Lohan, 2003; Tebo et al., 2004). The poor correlation

between Al and Mn in all our stations (from north to south, $r = 0.57$ at ES1000, 0.22 at GA1000, and 0.35 at AL1000) supports this view (Supplementary Table 2). Fe strongly correlates with Al in the Escombreras and Almeria canyons, with $r > 0.91$ and $p < 0.01$ (Supplementary Table 2), thus pointing to a lithogenic source and/or shared distributions. On the contrary, in the Garrucha-Almanzora Canyon system there is a poor correlation ($r = 0.48$) between Fe and Al, but a better Fe correlation with Mn, with $r = 0.67$ and $p < 0.05$ (Supplementary Table 2). Therefore, Fe contents in the Garrucha-Almanzora Canyon system likely respond to the presence of particle sources other than just lithogenic.

In the next subsections, we use the PCA results to assess TMs variability on a canyon by canyon basis.

5.2.1. Escombreras Canyon

The first component in the Escombreras Canyon would reflect an authigenic component, which explains most of the variance of Co, Cu, Mn, Ni and, to a lesser extent, As and Zn, during the six-monthly monitoring period (Fig. 3a and Supplementary Table 2). The scavenging behavior of these metals onto Mn (oxy)hydroxides (Huang and Conte, 2009) and/or the oxidation of dissolved species leading to the precipitation of oxides (e.g. Co oxides) that behave similarly to Mn oxides (Dulaquais et al., 2017) could explain the above association. Authigenic component scores displayed a clear trend with the minima in March and April, concomitantly with the storm events, with maximum values in summer months. This suggests that variability arises partly from changes in particle sources between the two periods, likely as a result of resuspension over the shelf and subsequent downward transport in the first period, and of disconnection from the shelf and dominating pelagic sedimentation during the second period.

The second component is clearly lithogenic as it describes most of the temporal variance of Al, Fe, Ti and, to a lesser extent, Ni and OM, with modulation by $CaCO_3$ inputs accounting for a negative loading. However, most of the temporal variance of Pb is largely captured within a third component, which is also contributed by other TMs such as As, Co, Cu and Zn, which may derive from anthropogenic sources. This third component displays negative scores in March and April 2015 and positive scores during summer months.

5.2.2. Garrucha-Almanzora Canyon system

We interpret the first component to reflect authigenic Mn and Fe bearing phases, such as oxides and oxidized particle coatings. The PCA results (Fig. 3b) and the close correlation of particulate As, Co, Cu and Pb with Mn (from $r = 0.68$, $p < 0.05$ for Pb to $r = 0.88$, $p < 0.01$ for As), and of Co and Cu with Fe ($r > 0.83$, $p < 0.01$) (Supplementary Table 2) indicate a joint transport into the canyon. This component depicts strong scores after May, and positive scores during June and early July, when anthropogenic disturbances can be a major driver of TMs transfer into the canyon axis (cf. section 5.1). Seafloor disturbance is able to release metals from bottom sediments to the water column (Eggleton and Thomas, 2004; Kalnejais et al., 2007; Bancon-Montigny et al., 2019), which then could be re-absorbed onto floating particles following resuspension events (Rusiecka et al., 2018; Al-Hashem et al., 2022).

The negative relationship between TMF and the contents of the above-mentioned TMs (Supplementary Fig. 2) suggests that dilution processes could have played a role in the observed temporal fluctuations. Yet, little is known about the role of bottom trawling in the TMs fate and redistribution (Palanques et al., 2022). Any geographical shift of resuspension area, and/or a change in particle loads and their properties (grain size, composition) or in oxygen content of the bottom water hold the potential to impact metal contents in resuspended particles forming nepheloid layers (Lohan and Bruland, 2008; Palanques et al., 2022) and, therefore, in the sinking fluxes.

The second component describes the lithogenic fraction, explaining most of Al, Ni and, to a lesser extent, Co and Fe variance (31% of individual variance) (Fig. 3b). Zn and Pb mostly bivariate together, thus contributing to a fourth component.

5.2.3. Almeria Canyon

The first component primarily reflects the influence of biogenic (OM) and authigenic Mn (oxy)hydroxides, and explains a significant portion of the variance of Co, Cu, Mn, Ni and, to a smaller extent, Zn and OM. Scores associated with this component noticeably increased after April 2015, reaching their maximum during summer months, from where they remained slightly positive until late autumn (Fig. 3c). During summer period, the above contributions were not masked by components that otherwise dominate mass fluxes in resuspended material, thus resembling Escombreras Canyon.

The second component is indicative of the lithogenic fraction, and accounts for most of Al, Fe and Ti variance and, to a lower extent, As and Ni. Interestingly, the autumn months displayed stronger positive scores and high Al and Fe contents (Fig. 2b), which could relate to the likely arrival to the site of terrestrial material after a November flood of the Andarax River. The enhancement of lithogenic inputs following fluvial discharges in the Alboran Sea has been previously reported (Fabres et al., 2002; Sanchez-Vidal et al., 2004). TM contents were modulated by $CaCO_3$ biogenic inputs (Fig. 3c). As mentioned in section 4.1, $CaCO_3$ inputs into this canyon seem to correspond mostly to pelagic settling from the overlaying water column, with a diminution of the relative abundance of lithogenics during late summer. However, $CaCO_3$ contents were also enhanced by resuspended and laterally advected material during the storm events, at the beginning and the end of the study period (Fig. 2b). The two principal components did not account for much of Pb and Zn interannual variability, as observed for the other two canyons (Fig. 3c).

5.2.4. Common features amongst canyons

Our results indicate the three investigated canyons share a number of features. Authigenic Mn (oxy)hydroxides played a key role in most of As, Co, Cu, Mn and Ni interannual variance (Fig. 3). Particulate Mn contents relate to its predisposition for oxidative precipitation. River discharges, shelf sediment resuspension and diffusion from the seafloor are likely sources of dissolved Mn and Fe into the water column (Marin and Giresse, 2001; Noble et al., 2012; Dulaquais et al., 2017), which can subsequently precipitate onto suspended particles while co-scavenging other dissolved TMs. This would be especially the case of dissolved Mn, which slow kinetic rates of oxidation (Jensen et al., 2020) and easiness to form complexes with organic ligands (Oldham et al., 2017) promote Mn transport to deeper environments (Jensen et al., 2020), such as the Escombreras and Almeria canyons. The width of the continental shelf, together with bottom oxygen concentrations and acting physical processes, can influence the seaward transport of dissolved Mn (Noble et al., 2012). As for the Garrucha-Almanzora Canyon system, our results suggest that Fe oxides also contributed to the authigenic fraction, implying additional processes, such as benthic resuspension as a likely prevalent source of redox sensitive TMs.

The lithogenic contribution to TMs interannual variance was especially relevant for Al, Fe (though less in GA1000 station) and Ti. Nevertheless, it did not account for the variance of most of the other TMs (Fig. 3). This could be viewed as surprising as this fraction dominated mass fluxes in all three canyons. Certainly, it was the responsible of most of the temporal variance of Ni and Co in GA1000 (61 and 42% of the total variance, respectively), as observed after PC2 scores (Fig. 3b). In contrast, the poor association of TMs with OM (PC3) (Fig. 3a) suggests a minor biogenic contribution to TMs export. The near-bottom placement of our sediment traps could have hampered observing potential associations of TMs' export with biological carriers, as the redistribution and dissolution of metals in sinking particles weaken such relationships with depth (Huang and Conte, 2009; Blain et al., 2022). It should be, however, noticed that the statistical analysis in our study tends to highlight the phase to which each TM is mainly associated to, and also that to a greater or lesser extent, most TMs are coupled with multiple types of particles (Huang and Conte, 2009; Conte et al., 2019). Finally, it's worth noting that Pb and Zn's intraannual variation in all three canyons was

captured by other components, which likely reflect anthropogenic contributions, possibly from several introductory pathways, including atmospheric deposition, thus further increasing the poor correlation of these metals with the main fractions and the other TMs.

Fig. 4 shows a generalized impoverishment of TM contents and metals representing the authigenic and lithogenic fractions (excluding Ti) at the occasion of the spring 2015 and winter 2016 storms in the Escombreras and Almeria canyons. Settling particles from the Garrucha-Almanzora Canyon system exhibited much less marked differences, in terms of TMs contents, between periods with and without storms compared to the other two canyons (Fig. 4). The larger compositional shifts between calm and stormy conditions for Zn, Ni, Mn, Fe and Al occur in Almeria Canyon, with e.g. mean values from 1162.4 ± 64.9 down to 848.9 ± 53.5 μg g^{-1} for Mn. For Co and Cu the larger differences correspond to Escombreras Canyon. For As the step between the two periods —calm vs. stormy— is almost equal in Escombreras and Almeria canyons (Fig. 4).

The above suggest that storm events led to the export of resuspended material from the adjacent shelves, which only reached the deep canyon environment during such energetic processes. Both the authigenic Mn oxides and the detrital fractions appeared to be diluted in those laterally advected sediments. Dilution was evident not only in the authigenic fraction but also in the detrital fraction, which dominates the resuspended material on continental margins. An explanation could be that the resuspended material was primarily enriched in $CaCO_3$, as illustrated in Fig. 2c and 3a, c. This view is in agreement with observations in the northwestern Mediterranean margin during high energy events (Cossa et al., 2014). However, in the investigated canyons we did not observe a correlation between grain size and TMs, which would be largely due to the small variation in the fluxes grain size throughout the monitoring period. While storms may have generated bottom shear stress capable of remobilizing coarse sediments on the shelves, the prevailing currents were likely not sufficient to carry a coarser suspended load till reaching the locations of the mooring stations.

5.3. Trace metals distributions in the submarine canyons

We observe regional variations in spatial TMs distributions. The Almeria Canyon commonly displays higher TM contents (Fig. 2b) than the Escombreras Canyon and the Garrucha-Almanzora Canyon system to the north. Variance analysis indicates that they are significantly different at a $p < 0.05$ level, except for As and Co from the Escombreras and Almeria stations (see statistical parameters in Table 1). The lower contents of detrital $CaCO_3$ in the particles of the margin segment to the south —where Almeria Canyon is located— compared to the northern margin segments (Tarrés et al., 2022) can explain the differences in Al, Fe, Ti and other TM contents. This observation fits with the fact that minerals from terrestrial sources are a relevant constituent of particle standing stocks and bottom sediments in continental marginal settings. This would ultimately relate to inland geology, which determines the composition of the sedimentary particles feeding the continental margin as a result of weathering processes and sediment transport by surface run-off and fluvial discharge.

When normalized to Al, the differences in TM concentrations between sampling stations in the northern and the southern margin segments diminish. This allows grouping the investigated canyons in two clusters: (i) Almeria and Escombreras canyons have high normalized ratios of As, Cu, Co and Mn in settling particles, and (ii) the Garrucha-Almanzora Canyon system has lower normalized ratios of the previous elements in settling particles. This results from distinct TMs cycling and

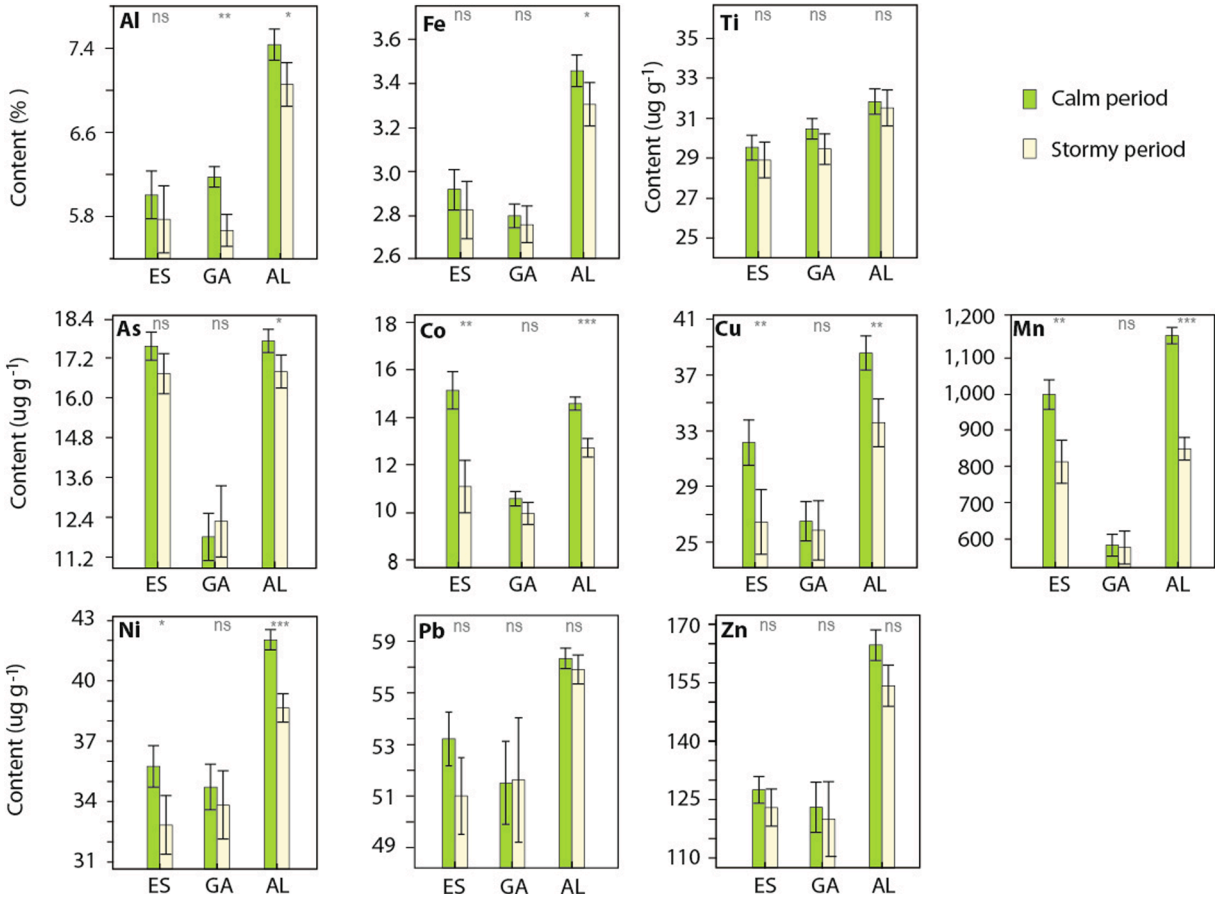

Fig. 4. Metal contents in settling particles during calm and stormy periods from March 2015 to March 2016 in Escombreras Canyon (ES), Garrucha-Almanzora Canyon system (GA) and Almeria Canyon (AL). Significance of the variance (p-values): *$p < 0.05$, ** $p < 0.01$, ***$p < 0.001$. ns: non-significant.

fate in the Garrucha-Almanzora Canyon system respect the other canyons (cf. section 5.2).

5.4. Modification of trace metal contents in canyon floors

So far we have discussed the distributions of TMs in the settling particles. Whereas the ultimate fate for sinking particle fluxes is the seafloor, the bulk composition of bottom sediments often differs from the one of settling particles in the water column, a situation that has been attributed to post-depositional processes, changes of particle sources, and alteration of the primary fluxes in the water column (Tesi et al., 2010; Raiswell, 2011; Heimbürger et al., 2012; Thibault de Chanvalon et al., 2016). We address this issue by comparing the TWC obtained for the study period with the canyon floor sediments of Escombreras Canyon and Garrucha-Almanzora Canyon system. We are obviously aware that even a single centimetre of bottom sediments can encompass years of deposition.

We calculated the TM in excess of seafloor sediments after the TWC of settling particles, both normalized and non-normalized to Al as a proxy for grain size (Table 2). The peak value for seafloor excess of Mn (65.4 %) appears at ES1000, while the one for Fe (20.7 %) occurs at GA1000. Such excess Mn and Fe could be associated to early diagenetic processes involving the reduction of Fe-Mn oxides in sub-oxic horizons and the diffusion of the dissolved Fe and Mn towards the sediment–water interface followed by re-precipitation in the redox boundary (Calvert and Price, 1972; Froelich et al., 1979; Marin and Giresse, 2001). After such a cycling in the sediment, resuspension and transport processes could transfer these phases by advection over the seabed (Sanchez-Vidal et al., 2005; Lee et al., 2018), as described in section 3.2. The excess Ti (24.2%) in surficial sediments of the Garrucha-Almanzora Canyon system compared to Escombreras Canyon (-8.2%) could indicate differential resuspension processes and near-bottom transport from one canyon to the other. It is well known that Ti preferentially concentrates in the coarser fractions of the sediment together with other heavy minerals such as titanomagnetite, ilmenite, augite and rutile (Boyle, 1983). It is plausible that the excess Fe in the Garrucha-Almanzora Canyon system also results from near-bottom processes, as it occurs for some heavy minerals (Dill, 2007).

After normalizing TM concentrations to grain size, the rather similar values (less than ± 10% of excess) for most of them (Table 2) suggest that metal excesses in the sediment could be partially explained by differences in grain size. Excesses higher than 25% for As in the Escombreras Canyon floor, and for Pb in the Garrucha-Almanzora Canyon system floor (Table 2) could be explained by diagenetic remobilization related to the excess of redox-sensitive Mn. This process would provide a plausible explanation for the distribution of As in Escombreras Canyon (Chaillou et al., 2003), with sulfate reducing bacteria possibly playing a role according to recent findings by Baza-Varas et al. (2023). Elevated Pb contents in the Garrucha-Almanzora Canyon system can result from in-situ suboxic diagenetic remobilization too (El Houssainy et al., 2020) and/or from reabsorption onto benthic resuspended particles (Rusiecka et al., 2018) and posterior deposition. Additionally, As, Co, Cu and Mn show moderate increases in bottom sediments. The PCA indicates that the distribution of Cu, Co, As, and Pb in the sediment is linked to the presence of Fe and Mn oxides (Fig. 3b). The Garrucha-Almanzora Canyon system apparently being a dynamic setting, with bottom resuspension and lateral advection, is consistent with the observed Ti enrichment of seafloor sediments. Thus, resuspension and near-bottom transport are probably able to modify the geochemical composition of the canyon' floor.

5.5. The anthropogenic imprint on trace metal contents in deep submarine canyons

The distribution and cycling of TMs in the sediments of the study area and similar settings are likely modified by anthropogenic activities. Increments in TM contents in continental slope environments, including submarine canyons, due to anthropogenic activities have been previously reported (e.g., Palanques et al., 2008; Richter et al., 2009; Jesus et al., 2010; Costa et al., 2011; Mil-Homens et al., 2013b; Cossa et al., 2014; Roussiez et al., 2012; Heimbürger et al., 2012; Azaroff et al., 2020). The EFs approach uses pre-industrial sediments encompassing several years of deposition as normalizers. The estimation of EFs for each individual trap sample could incorporate a bias due to the different time periods represented by the normalizing sediments. This relates to the fact that, after correction for the terrigenous fraction, enrichments could result from several processes that enhance TM concentrations beyond anthropogenic inputs, such as biological uptake or authigenic precipitation (Yiğiterhan et al., 2011). In practice, we have considered TWC > 1.5 as an indicator of anthropogenic inputs, as this value represents the natural variability threshold following Roussiez et al. (2006), Radakovitch et al. (2008), and Jesus et al. (2010). The normalization of metal contents to pre-industrial values reveals a moderate enrichment of Zn and Cu, with mean values of up to 1.7 for Zn in Escombreras Canyon, and 1.5 and 1.6 for Cu in Garrucha-Almanzora Canyon system and Almeria Canyon, respectively (Fig. 5). The range of values from 0.75 to 1.5 is normally considered within natural variability (Radakovitch et al., 2008). However, one can note that Pb and Cu almost exceed the natural threshold in Escombreras Canyon, and Zn does the same in the other two canyons. The values obtained for canyon floor sediments tend to be in the interquartile range of the box plot, indicating that the trapped material provides a good record of TM pollutants being buried there. One exception are the metals affected by diagenetic and/or other near-bottom processes as discussed in section 5.3, which include As and Pb in the ES1000 and GA1000 stations, respectively.

The provinces of Murcia and Almeria experienced a noticeable industrial development during the second half of the 20th century. The region has an intensive farming model, with one of the largest areas in Europe dedicated to greenhouse agriculture along the coastline of the southern margin segment here investigated. Beyond rich agricultural expanses not far from shore, the northern margin segment hosts an important petrochemical industrial complex of Escombreras, which is besides the coastal town of Cartagena and<6 km west of Portman Bay. The complex started its activities in 1950 and since then has experienced several enlargements. Further environmental stressors arise from sewage pipes along the coastline discharging into the sea wastes from industrial activities, ancient ponds and dumping sites filled with industrial and mining wastes, and the traffic of tankers and cargo vessels. Portman Bay actually constitutes one of the main environmental disasters along the European coastline. This bay was used during>30 years as the dumping site for huge amounts of Pb, Zn, Cu, As and other metals rich mine tailings from the open pit exploitation of sulphide ores (Fig. 1) (Baza-Varas et al., 2022, and references therein). Although waste disposal ended in 1990, the mine tailings disposed in the coastal sea remains nowadays. Previous studies have shown high levels of TMs pollution across the modern inner shelf floor off Portman Bay (Alorda-Kleinglass et al., 2019; Cerdà-Domènech et al., 2020), altogether with a diminishing sedimentation rate farther offshore in the tailings deposit itself (Baza-Varas et al., 2022).

Cu contents exceed or are near the pre-industrial threshold in all canyons, which points to a widespread contamination (Fig. 5). In other areas, Cu contamination has been mostly related to spillages attributed to the use of fungicides or fertilizers in agriculture (Roussiez et al., 2012; Cossa et al., 2014) or waste water treatment plants (Casadevall et al., 2016). Zn reaches contamination levels only in the Escombreras Canyon (Fig. 5), which is the closest to the Escombreras petrochemical complex and to Portmán Bay of the three studied canyons. The offshore extension of Portman Bay mine tailings deposit (see Baza-Varas et al., 2023), at about 13 km in straight line from ES1000 (Fig. 1), seems a good candidate for Zn and other TMs (Cu and Pb) sourcing to the adjacent continental slope and canyons. Zn enrichment would decrease progressively with increasing distance from Portman's dumping site by

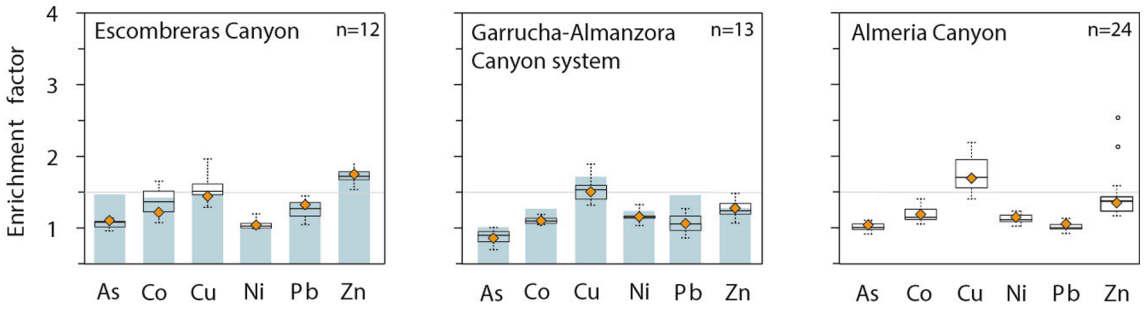

Fig. 5. Trace metals enrichment factors (EFs) in setting particles in the investigated submarine canyons. The dashed horizontal line represents the natural variability threshold after Roussiez et al. (2006). White dots represent the outliers (in the present case abnormal high values relative to the co-existing data). The orange diamonds illustrate the EFs for TWC whereas the blue grey columns represent EFs in canyon floor sediments. Note that no bottom sediments were available for Almeria Canyon (cf. section 2.1). (For interpretation of the references to color in this figure legend, the reader is referred to the web version of this article.)

mixing with non-enriched particles and dilution. However, we cannot discard other potential sources such as hydrocarbon burning at Escombreras complex or the onshore contaminated sites that could release pollutants able to reach the outer continental margin via atmospheric inputs. In the case of Zn for the rest of canyons, the results of the PCA show that its temporal variation is independent of the rest of the elements, possibly stemming from anthropogenic factors. However, it is associated with Pb, which does not exhibit high EF (Fig. 3c).

The anthropogenic imprint on submarine canyons in the Iberian Atlantic margin and the SW and NW Mediterranean Sea, in terms of TM enrichment, is illustrated in Fig. 6a. Source type, distance from source and transport pathways and their carrying capacity determine which TM pollutants and amounts may reach the deep continental margin. For instance, the Planier Canyon shows a specific signature due to local inputs from a bauxite treatment plant on the shore (Roussiez et al., 2012). Furthermore, hydrodynamics and sedimentary dynamics in each specific continental margin segment also influence the transference of the TM pollutants, as illustrated by higher Pb values in Atlantic canyon

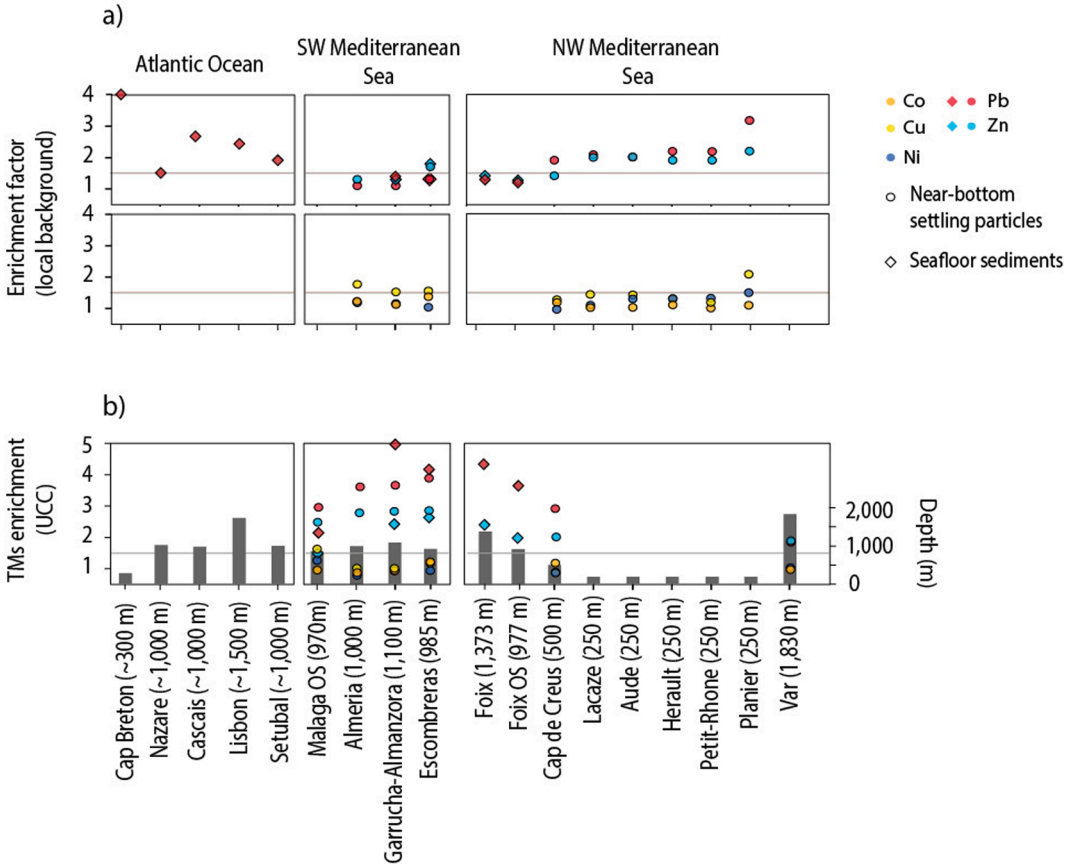

Fig. 6. Compilation of trace metals (TMs) mean enrichments from submarine canyons and nearby open slopes from Iberian Atlantic and NW Mediterranean continental margins altogether with those from the SW Mediterranean margin, where the investigated canyons lie. (a) Enrichment factors (EFs) calculated with respect to local background pre-industrial values, and (b) enrichment values with respect the Upper Continental Crust (UCC) global average composition according to Rudnick and Gao (2003). The general location of the canyons in the plot is shown in Fig. 1a. OS: open slope. Malaga OS corresponds to ALB1 station in the Alboran Sea, for which data have not been published previously (see detailed location in Sanchez-Vidal et al., 2005). Water depths in meters are given in brackets for each sampling station. Data are from Azaroff et al. (2020) for Cap Breton Canyon; Jesus et al. (2010) for Nazare, Cascais, Lisbon and Setubal canyons; Palanques et al. (2008) for the Foix Canyon and OS; Cossa et al. (2014) for Cap de Creus Canyon; Roussiez et al. (2012) for Lacaze, Aude, Herault, Petit-Rhone and Planier canyons; and Heimbürger et al. (2012) for Var Canyon. The horizontal lines denote the natural variability threshold after Roussiez et al. (2006).

floor sediments (Fig. 6a) (Jesus et al., 2010).

The choice of the reference material for the calculation of EFs is critical to correctly assess metal enrichment levels. Fig. 6 compares the mean EFs resulting from using pre-industrial sediments as local background. We have also considered in Fig. 6 formerly reported TMs enrichments in sediments from different locations and water depths in submarine canyons and open slopes around the Iberian Peninsula and nearby areas against the composition of the upper continental crust (UCC) as obtained from Rudnick and Gao (2003). The values calculated after the UCC global average exceed EFs calculated after the local pre-industrial background, thus illustrating that the use of UCC composition as reference value may result in an inaccurate, exaggerated view of the degree of TM pollution (Fig. 6b). This is well illustrated in the Portman area, where there is a natural geochemical anomaly for Pb, Zn and As that directly relates to local geology (López-García et al., 2017). Anthropogenic enrichments are, therefore, seen when local reference values are taken into account.

6. Conclusions

The transport and sink of TMs in SW Mediterranean submarine canyons depend on a number of physical and biogeochemical processes, and nowadays are also affected by anthropogenic perturbations (i.e. spillage of chemicals used in agriculture, industrial emissions via atmospheric transport, and/or past mining activities). TM contents in downward particle fluxes rely upon the composition and amounts of detrital material reaching the continental margin, on scavenging into Mn oxides, and on anthropogenic inputs. Besides the dominant particulate carriers of TMs described in this study, it is likely that further biological interactions during transport influence TM cycling anyhow. Anthropogenic sources would result in excess Zn in Escombreras Canyon and excess Cu in all the studied canyons. The widespread Cu enrichment suggests a diffuse source such as intensive farming activities in the coastal area and watershed, whereas Zn enrichment in the northern Escombreras Canyon points to local industrial activities. Yet, one possible source could be the export of Zn and other TMs, such as Cu and Pb, from the underwater extension of Portman's mine tailings deposit from sulphide ore exploitation, located at about 13 km from the canyon head. Whereas the shelf edge spillover of TMs and other pollutants is a rather common phenomenon, the calculation of EFs requires a correct choice of the reference materials to be used, prioritizing the local ones.

Storm events enhance downward TM fluxes into the submarine canyons, though concentrations are generally less than in fluxes under calm conditions. This is attributed to a dilution effect of the TMs enriched particles exported during the calm periods within the resuspended shelf material exported during stormy periods. However, seasonal or event-driven changes in sinking fluxes are barely observed in the Garrucha-Almanzora Canyon system, where a more steady TMs export through time has been observed. The content and transport of As, Co, Cu and Pb into the canyon seems to be instead influenced by bottom resuspension and advective transport of Mn and Fe bearing phases, with bottom trawling likely playing a non-negligible role. Further, the rather high Ti and Fe contents in the canyon's floor indicate differential resuspension according to particles' density.

The spreading of bottom trawling points to the need of specific studies to better understand how this activity influences TM fluxes within settling particles in submarine canyons and other deep-sea settings.

Declaration of Competing Interest

The authors declare that they have no known competing financial interests or personal relationships that could have appeared to influence the work reported in this paper.

Data availability

Data will be made available on request.

Acknowledgements

We would like to express our gratitude to the many colleagues and technicians and to the crew of RV Ángeles Alvariño for their support during sea-going work. We also thank M. Guart and F. Menéndez for their assistance in the lab and J. Martín for his comments on the manuscript. This research was supported by research projects NUREIEV (ref. CTM2013-44598-R) and NUREIEVA (ref. CTM2016-75953-C2-1-R) funded by the Spanish Ministry of Economy and Competitiviness (MINECO), and the Spanish Ministry of Economy, Industry and Competitiviness (MINECO), respectively. GRC Geociències Marines is funded by the Catalan Government within its excellence research groups program (ref. 2021 SGR 01195). M. Tarrés was supported by a FPI grant from the Spanish Ministry of Science and Innovation (MICINN).

Appendix A. Supplementary material

Supplementary data to this article can be found online at https://doi.org/10.1016/j.pocean.2023.103122.

References

Acosta, J., Fontán, A., Muñoz, A., Muñoz-Martín, A., Rivera, J., Uchupi, E., 2013. The morpho-tectonic setting of the Southeast margin of Iberia and the adjacent oceanic Algero-Balearic Basin. Mar. Pet. Geol. 45, 17–41. https://doi.org/10.1016/j.marpetgeo.2013.04.005.

Al-Hashem, A.A., Beck, A.J., Krisch, S., Menzel Barraqueta, J.-L., Steffens, T., Achterberg, E.P., 2022. Particulate trace metal sources, cycling, and distributions on the southwest African shelf. Glob. Biogeochem. Cycles 36. https://doi.org/10.1029/2022GB007453.

Alorda-Kleinglass, A., Garcia-Orellana, J., Rodellas, V., Cerdà-Domènech, M., Tovar-Sánchez, A., Diego-Feliu, M., Trezzi, G., Sánchez-Quilez, D., Sanchez-Vidal, A., Canals, M., 2019. Remobilization of dissolved metals from a coastal mine tailing deposit driven by groundwater discharge and porewater exchange. Sci. Total Environ. 688, 1359–1372. https://doi.org/10.1016/j.scitotenv.2019.06.224.

Aloupi, M., Angelidis, M.O., 2001. Normalization to lithium for the assessment of metal contamination in coastal sediment cores from the Aegean Sea. Mar. Environ. Res. 52, 1–12. https://doi.org/10.1016/S0141-1136(00)00255-5.

Anderson, R.F., 2020. GEOTRACES: Accelerating research on the marine biogeochemical cycles of trace elements and their isotopes. Annu. Rev. Mar. Sci. 12 (1), 49–85. https://doi.org/10.1146/annurev-marine-010318-095123.

Anderson, R.F., Hayes, C.T., 2015. Characterizing marine particles and their impact on biogeochemical cycles in the GEOTRACES program. Prog. Oceanogr. 133, 1–5. https://doi.org/10.1016/j.pocean.2014.11.010.

Azaroff, A., Miossec, C., Lanceleur, L., Guyoneaud, R., Monperrus, M., 2020. Priority and emerging micropollutants distribution from coastal to continental slope sediments: A case study of Capbreton Submarine Canyon (North Atlantic Ocean). Sci. Total Environ. 703, 135057 https://doi.org/10.1016/j.scitotenv.2019.135057.

Bancon-Montigny, C., Gonzalez, C., Delpoux, S., Avenzac, M., Spinelli, S., Mhadhbi, T., Mejri, K., Hlaili, A.S., Pringault, O., 2019. Seasonal changes of chemical contamination in coastal waters during sediment resuspension. Chemosphere 235, 651–661. https://doi.org/10.1016/j.chemosphere.2019.06.213.

Baza-Varas, A., Canals, M., Frigola, J., Cerdà-Domènech, M., Rodés, N., Tarrés, M., Sanchez-Vidal, A., the NUREIEVA-MAR1 shipboard party, 2022. Multiproxy characterization of sedimentary facies in a submarine sulphide mine tailings dumping site and their environmental significance: the study case of Portmán Bay (SE Spain). Sci. Total Environ. 810, 151183. https://doi.org/10.1016/j.scitotenv.2021.151183.

Baza-Varas, A., Roqué-Rosell, J., Canals, M., Frigola, J., Cerdà-Domènech, M., Sanchez-Vidal, A., Amblàs, D., Campeny, M., Marini, C., 2023. As and S speciation in a submarine sulfide mine tailings deposit and its environmental significance: the study case of Portmán Bay (SE Spain). Sci. Total Environ. 882, 163649. https://doi.org/10.1016/j.scitotenv.2023.163649.

Birch, G.F., 2017. Determination of sediment metal background concentrations and enrichment in marine environments – A critical review. Sci. Total Environ. 580, 813–831. https://doi.org/10.1016/j.scitotenv.2016.12.028.

Blain, S., Planquette, H., Obernosterer, I., Guéneuguès, A., 2022. Vertical flux of trace elements associated with lithogenic and biogenic carrier phases in the Southern Ocean. Glob. Biogeochem. Cycles 36. https://doi.org/10.1029/2022GB007371.

Boyle, E.A., 1983. Chemical accumulation variations under the Peru Current during the past 130,000 years. Geophys. Res. 88, 7667–7680. https://doi.org/10.1029/JC088iC12p07667.

Bradshaw, C., Tjensvoll, I., Sköld, M., Allan, I.J., Molvaer, J., Magnusson, J., Naes, K., Nilsson, H.C., 2012. Bottom trawling resuspends sediment and releases bioavailable

contaminants in a polluted fjord. Environ. Pollut. 170, 232–241. https://doi.org/10.1016/j.envpol.2012.06.019.
Bruland, K.W., Lohan, M.C., 2003. Controls of trace metals in seawater. In: Holland, H. D., Turekian, K.K. (Eds.), Treatise on Geochemistry, Vol. 6. Elsevier, Amsterdam, pp. 23–47. https://doi.org/10.1016/B0-08-043751-6/06105-3.
Calvert, S.E., Price, N.B., 1972. Diffusion and reaction profiles of dissolved manganese in the pore waters of marine sediments. Earth Planet. Sci. Lett. 16 (2), 245–249. https://doi.org/10.1016/0012-821X(72)90197-5.
Casadevall, M., Torres, J., El Aoussimi, A., Carbonell, A., Delgado, E., Sarrà-Alarcón, L., García-Ruíz, C., Esteban, A., Mallol, S., Bellido, J.M., 2016. Pollutants and parasites in bycatch teleosts from south eastern Spanish Mediterranean's fisheries: concerns relating the foodstuff harnessing. Mar. Pollut. Bull. 104, 182–189. https://doi.org/10.1016/j.marpolbul.2016.01.040.
Cerdà-Domènech, M., Frigola, J., Sanchez-Vidal, A., Canals, M., 2020. Calibrating high resolution XRF core scanner data to obtain absolute metal concentrations in highly polluted marine deposits after two case studies off Portmán Bay and Barcelona. Spain. Sci. Total Environ. 717, 134778 https://doi.org/10.1016/j.scitotenv.2019.134778.
Chaillou, G., Schäfer, J., Anschutz, P., Lavaux, G., Blanc, G., 2003. The behaviour of arsenic in muddy sediments of The Bay of Biscay (France). Geochim. Cosmochim. Acta 67 (16), 2993–3003. https://doi.org/10.1016/S0016-7037(03)00204-7.
Charette, M.A., Lam, P.J., Lohan, M.C., Kwon, E.Y., Hatje, V., Jeandel, C., Shiller, A.M., Cutter, G.A., Thomas, A., Boyd, P.W., Homoky, W.B., Milne, A., Thomas, H., Andersson, P.S., Porcelli, D., Tanaka, T., Geibert, W., Dehairs, F., Garcia-Orellana, J., 2016. Coastal ocean and shelf-sea biogeochemical cycling of trace elements and isotopes: lessons learned from GEOTRACES. Philosophical Transactions of the Royal Society A 374, 20160076. https://doi.org/10.1098/rsta.2016.0076.
Conte, M.H., Carter, A.M., Koweek, D.A., Huang, S., Weber, J.C., 2019. The elemental composition of the deep particle flux in the Sargasso Sea. Chem. Geol. 511, 279–313. https://doi.org/10.1016/j.chemgeo.2018.11.001.
Cossa, D., Buscail, R., Puig, P., Chiffoleau, J.-F., Radakovitch, O., Jeanty, G., Heussner, S., 2014. Origin and accumulation of trace elements in sediments of the northwestern Mediterranean margin. Chem. Geol. 380, 61–73. https://doi.org/10.1016/j.chemgeo.2014.04.015.
Costa, A.M., Mil-Homens, M., Lebreiro, S.M., Richter, T.O., de Stigter, H., Boer, W., Trancoso, M.A., Melo, Z., Mouro, F., Mateus, M., Canário, J., Branco, V., Caetano, M., 2011. Origin and transport of trace metals deposited in the canyons off Lisboa and adjacent slopes (Portuguese Margin) in the last century. Mar. Geol. 282, 169–177. https://doi.org/10.1016/j.margeo.2011.02.007.
Cowen, J.P., Bruland, K.W., 1985. Metal deposits associated with bacteria: implications for Fe and Mn marine biogeochemistry. Deep Sea Res. Part I Oceanogr. Res. Pap. 32 (3), 253–272. https://doi.org/10.1016/0198-0149(85)90078-0.
Dill, H.G., 2007. Grain morphology of heavy minerals from marine and continental placer deposits, with special reference to Fe–Ti oxides. Sed. Geol. 198 (1–2), 1–27. https://doi.org/10.1016/j.sedgeo.2006.11.002.
Dulaquais, G., Planquette, H., L'Helguen, S.M.J., Rijkenberg, A., Boye, M., 2017. The biogeochemistry of cobalt in the Mediterranean Sea. Glob. Biogeochem. Cycles 31, 377–399. https://doi.org/10.1002/2016GB005478.
Dumas, C., Aubert, D., Durrieu de Madron, X., Ludwig, W., Heussner, S., Delsaut, N., Menniti, C., Sotin, C., Buscail, R., 2014. Storm-induced transfer of particulate trace metals to the deep-sea in the Gulf of Lion (NW Mediterranean Sea). Environ. Geochem. Health 36, 995–1014. https://doi.org/10.1007/s10653-014-9614-7.
Durrieu de Madron, X., Aubert, D., Charrière, B., Kunesch, S., Menniti, C., Radakovitch, O., Sola, J., 2023. Impact of Dense Water Formation on the Transfer of Particles and Trace Metals from the Coast to the Deep in the Northwestern Mediterranean. Water (15), 301. https://doi.org/10.3390/w15020301.
Eggleton, J., Thomas, K.V., 2004. A review of factors affecting the release and bioavailability of contaminants during sediment disturbance events. Environ. Int. 30 (7), 973–980. https://doi.org/10.1016/j.envint.2004.03.001.
El Houssainy, A., Abi-Ghanem, C., Dang, D.H., Mahfouz, C., Omanović, D., Khalaf, G., Mounier, S., Garnier, C., 2020. Distribution and diagenesis of trace metals in marine sediments of a coastal Mediterranean area: St Georges Bay (Lebanon). Mar. Pollut. Bull. 155, 111066. https://doi.org/10.1016/j.marpolbul.2020.111066.
El Khatab, M., 2006. Dinámica del material sedimentario y de los metales pesados asociados en el margen noroccidental del mar de Alborán. PhD Thesis. Universidad Politécnica de Cataluña, Barcelona, Spain, p. 269.
Fabres, J., Calafat, A., Sanchez-Vidal, A., Canals, M., Heussner, S., 2002. Composition and spatio-temporal variability of particle fluxes in the Western Alboran Gyre, Mediterranean Sea (SW Mediterranean). J. Mar. Syst. 33–34, 431–456.
Froelich, P.N., Klinkhammer, G.P., Bender, M.L., Luedtke, N.A., Heath, G.R., Cullen, D., Dauphin, P., Hammond, D., Hartman, B., 1979. Early oxidation of organic matter in pelagic sediments of the eastern equatorial Altantic: suboxic diagenesis. Geochim. Cosmochim. Acta 43, 1075–1090. https://doi.org/10.1016/0016-7037(79)90095-4.
Geibert, W., 2018. Processes that regulate trace element distribution in the ocean. Elements 14, 391–396. https://doi.org/10.2138/gselements.14.6.3912015.
Grousset, F.E., Quetel, C.R., Thomas, B., Donard, O.F.X., Lambert, C.E., Guillard, F., Monaco, A., 1995. Anthropogenic vs. lithogenic origins of trace elements (As, Cd, Pb, Rb, Sb, Sc, Sn, Zn) in water column particles: northwestern Mediterranean Sea. Mar. Chem. 48 (3–4), 291–310. https://doi.org/10.1016/0304-4203(94)00056-J.
Hanebuth, T.J.J., King, M.L., Mendes, I., Lebreiro, S., Lobo, F.J., Oberle, F.K., Antón, L., Ferreira, P.A., Reguera, M.I., 2018. Hazard potential of widespread but hidden historic offshore heavy metal (Pb, Zn) contamination (Gulf of Cadiz, Spain). Sci. Total Environ. 637–638, 561–576. https://doi.org/10.1016/j.scitotenv.2018.04.352.
Heimbürger, L.-E., Cossa, D., Thibodeau, B., Khripounoff, A., Mas, V., Chiffoleau, J.-F., Schmidt, S., Migon, C., 2012. Natural and anthropogenic trace metals in sediments of the Ligurian Sea (Northwestern Mediterranean). Chem. Geol. 291, 141–151. https://doi.org/10.1016/j.chemgeo.2011.10.011.
Heussner, S., Durrieu de Madron, X., Calafat, A., Canals, M., Carbonne, J., Delsaut, N., Saragoni, G., 2006. Spatial and temporal variability of downward particle fluxes on a continental slope: lessons from an 8-yr experiment in the Gulf of Lions (NW Mediterranean). Mar. Geol. 234, 63–92. https://doi.org/10.1016/j.margeo.2006.09.003.
https://emodnet.ec.europa.eu/geoviewer/: Interactive map viewer of the EMODnet server [last consulted 18th of April 2023].
Huang, S., Conte, M.H., 2009. Source/process apportionment of major and trace elements in sinking particles in the Sargasso sea. Geochim. Cosmochim. Acta 73, 65–90. https://doi.org/10.1016/j.gca.2008.08.023.
Hung, J.J., Ho, C.Y., 2014. Typhoon- and earthquake-enhanced concentration and inventory of dissolved and particulate trace metals along two submarine canyons off southwestern Taiwan. Estuar. Coast. Shelf Sci. 136, 179e190. https://doi.org/10.1016/j.ecss.2013.11.004.
Jeandel, C., Vance, D., 2018. New tools, new discoveries in marine geochemistry. Elements 14, 379–384. https://doi.org/10.2138/gselements.14.6.379.
Jensen, L.T., Morton, P., Twining, B.S., Heller, M.I., Hatta, M., Measures, C.I., John, S., Zhang, R., Pinedo-Gonzalez, P., Sherrell, R.M., Fitzsimmons, J.N., 2020. A comparison of marine Fe and Mn cycling: U.S. GEOTRACES GN01 Western Arctic case study. Geochim. Cosmochim. Acta 288, 138–160. https://doi.org/10.1016/j.gca.2020.08.006.
Jesus, C.C., de Stigter, H.C., Richter, T.O., Boer, W., Mil-Homens, M., Oliveira, A., Rocha, F., 2010. Trace metal enrichments in Portuguese submarine canyons and open slope: anthropogenic impact and links to sedimentary dynamics. Mar. Geol. 271 (1–2), 72–83. https://doi.org/10.1016/j.margeo.2010.01.011.
Kalnejais, L.H., Martin, W.R., Signell, R.P., Bothner, M.H., 2007. Role of sediment resuspension in the remobilization of particulate-phase metals from coastal sediments. Environ. Sci. Tech. 41, 2282–2288. https://doi.org/10.1021/es061770z.
Karageorgis, A.P., Katsanevakis, S., Kaberi, H., 2009. Use of enrichment factors for the assessment of heavy metal contamination in the sediments of Koumoundourou Lake, Greece. Water, Air, Soil Pollut. 204, 243–258. https://doi.org/10.1007/s11270-009-0041-9.
Kuss, J., Waniek, J.J., Kremling, K., Schulz-Bull, D.E. (2010). Seasonality of particle-associated trace element fluxes in the deep northeast Atlantic Ocean. Deep-Sea Res. I 57, 785–796. Doi: 10.1016/j.dsr.2010.04.002.
Lam, P.J., Bishop, J.K.B., Henning, C.C., Marcus, M.A., Waychunas, G.A., Fung, I.Y., 2006. Wintertime phytoplankton bloom in the subarctic Pacific supported by continental margin iron. Glob. Biogeochem. Cycles 20, GB1006. https://doi.org/10.1029/2005GB002557.
Lee, J.M., Heller, M.I., Lam, P.J., 2018. Size distribution of particulate trace elements in the U.S. GEOTRACES Eastern Pacific Zonal Transect (GP16). Mar. Chem. 201, 108–123. https://doi.org/10.1016/j.marchem.2017.09.006.
Lemaitre, N., Planquette, H., Dehairs, F., Planchon, F., Sarthou, G., Gallinari, M., Roig, S., Jeandel, C., Castrillejo, M., 2020. Particulate trace element export in the North Atlantic (GEOTRACES GA01 transect, GEOVIDE cruise). ACS Earth Space Chem. 4 (11), 2185–2204. https://doi.org/10.1021/acsearthspacechem.0c00045.
Lobo, F.J., Ercilla, G., Fernández-Salas, L.M., Gámez, D., 2014. The Iberian Mediterranean shelves. Geol. Soc. Lond. Mem. 41, 147–170. https://doi.org/10.1144/M41.11.
Lohan, M.C., Bruland, K.B., 2008. Elevated Fe(II) and dissolved Fe in hypoxic shelf waters off Oregon and Washington: an enhanced source of iron to coastal upwelling regimes. Environ. Sci. Technol. 42 (17), 6462–6468. https://doi.org/10.1021/es800144j.
López-García, J.A., Oyarzun, R., Lillo, J., Manteca, J.I., Cubas, P., 2017. Geochemical characterization of magnetite and geological setting of the iron oxide ± iron silicate ± iron carbonate rich Pb–Zn sulfides from the La Unión and Mazarrón stratabound deposits (SE Spain). Resour. Geol. 67 (2), 139–157. https://doi.org/10.1111/rge.12124.
Macias, D., Garcia-Gorriz, E., Stips, A., 2016. The seasonal cycle of the Atlantic Jet dynamics in the Alboran Sea: direct atmospheric forcing versus Mediterranean thermohaline circulation. Ocean Dyn. 2016 (66), 137–151. https://doi.org/10.1007/s10236-015-0914-y.
Marin, B., Giresse, P., 2001. Particulate manganese and iron in recent sediments of the Gulf of Lions continental margin (north-western Mediterranean Sea): deposition and diagenetic process. Mar. Geol. 172, 147–165. https://doi.org/10.1016/S0025-3227(00)00124-9.
Martín, J.H., Knauer, G.A., Gordon, R.M., 1983. Silver distribution and fluxes in the North-West Pacific waters. Nature 305, 306–309. https://doi.org/10.1038/305306a0.
Martín, J., Palanques, A., Puig, P., 2007. Near-bottom horizontal transfer of particulate matter in the Palamós Submarine Canyon (NW Mediterranean). J. Mar. Res. 65 (2), 193–218. https://doi.org/10.1357/002224007780882569.
Martín, J., Puig, P., Masqué, P., Palanques, A., Sánchez-Gómez, A., Vopel, K.C., 2014. Impact of bottom trawling on deep-sea sediment properties along the flanks of a submarine canyon. PLoS One 9 (8). https://doi.org/10.1371/journal.pone.0104536.
Mil-Homens, M., Blum, J., Canário, J., Caetano, M., Costa, A.M., Lebreiro, S.M., Trancoso, M., Richter, T., de Stigter, H., Johnson, M., Branco, V., Cesário, R., Mouro, F., Mateus, M., Boer, W., Melo, Z., 2013a. Tracing anthropogenic Hg and Pb input using stable Hg and Pb isotope ratios in sediments of the central Portuguese Margin. Chem. Geol. 336, 62–71. https://doi.org/10.1016/j.chemgeo.2012.02.018.
Mil-Homens, M., Caetano, M., Costa, A.M., Lebreiro, S., Richter, T., de Stigter, H., Trancoso, M.A., Brito, P., 2013b. Temporal evolution of lead isotope ratios in sediments of the Central Portuguese Margin: A fingerprint of human activities. Mar. Pollut. Bull. 74, 274–284. https://doi.org/10.1016/j.marpolbul.2013.06.044.

Mil-Homens, M., Vale, C., Naughton, F., Brito, P., Drago, T., Anes, B., Raimundo, J., Schmidt, S., Caetano, M., 2016. Footprint of roman and modern mining activities in a sediment core from the southwestern Iberian Atlantic shelf. Sci. Total Environ. 571, 1211–1221. https://doi.org/10.1016/j.scitotenv.2016.07.143.

Millot, C., 1999. Circulation in the Western Mediterranean Sea. J. Mar. Syst. 20 (1–4), 423–442. https://doi.org/10.1016/S0924-7963(98)00078-5.

Morel, F.M.M., Price, N.M., 2003. The biogeochemical cycles of trace metals in the oceans. Science 300, 944–947. https://doi.org/10.1126/science.1083545.

Noble, A.E., Lamborg, C.H., Ohnemus, D.C., Lam, P.J., Goepfert, T.J., Measures, C.I., Frame, C.H., Casciotti, K.L., DiTullio, G.R., Jennings, J., Saito, M.A., 2012. Basin-scale inputs of cobalt, iron, and manganese from the Benguela-Angola front to the South Atlantic Ocean. Limnol. Oceanogr. 57 (4), 989–1010. https://doi.org/10.4319/lo.2012.57.4.0989.

Ohnemus, D.C., Lam, P.J., 2015. Cycling of lithogenic marine particles in the US GEOTRACES North Atlantic transect. Deep Sea Res. Part II 116, 283–302. https://doi.org/10.1016/j.dsr2.2014.11.019.

Oldham, V.E., Miller, M.T., Jensen, L.T., Luther, G.W., 2017. Revisiting Mn and Fe removal in humic rich estuaries. Geochim. Cosmochim. Acta 209, 267–283. https://doi.org/10.1016/j.gca.2017.04.001.

Pagès, F., Martín, J., Palanques, A., Puig, P., Gili, J.M., 2007. High occurrence of the elasipodid holothurian Penilpidia ludwigi (von Marenzeller, 1893) in bathyal sediment traps moored in a western Mediterranean submarine canyon. Deep Sea Res. Part I 54, 2170–2180. https://doi.org/10.1016/j.dsr.2007.09.002.

Palanques, A., Masqué, P., Puig, P., Sanchez-Cabeza, J.A., Frignani, M., Alvisi, F., 2008. Anthropogenic trace metals in the sedimentary record of the Llobregat continental shelf and adjacent Foix Submarine Canyon (northwestern Mediterranean). Mar. Geol. 248, 213–227. https://doi.org/10.1016/j.margeo.2007.11.001.

Palanques, A., Paradis, S., Puig, P., Masqué, P., Lo Iacono, C., 2022. Effects of bottom trawling on trace metal contamination of sediments along the submarine canyons of the Gulf of Palermo (southwestern Mediterranean). Sci. Total Environ. 814, 152658 https://doi.org/10.1016/j.scitotenv.2021.152658.

Papale, M., Conte, A., Del Core, M., Zito, E., Sprovieri, M., De Leo, F., Rizzo, C., Urzì, C., De Domenico, E., Luna, G.M., Michaud, L., Lo Giudice, A., 2018. Heavy-metal resistant microorganisms in sediments from submarine canyons and the adjacent continental slope in the northeastern Ligurian margin (Western Mediterranean Sea). Prog. Oceanogr. 168, 155–168. https://doi.org/10.1016/j.pocean.2018.09.015.

Paradis, S., Goñi, M., Masqué, P., Durán, R., Arjona-Camas, M., Palanques, A., Puig, P., 2021. Persistence of biogeochemical alterations of deep-sea sediments by bottom trawling. Geophys. Res. Lett. 48 https://doi.org/10.1029/2020GL091279.

Parrilla, G., Kinder, T.H., Preller, R.H., 1986. Deep and intermediate Mediterranean water in the western Alboran Sea. Deep Sea Res., Part I Oceanogr. Res. Pap. 33, 55–88. https://doi.org/10.1016/0198-0149(86)90108-1.

Pérez-Hernández, S., Comas, M.C., Escutia, C., 2014. Morphology of turbidite systems within an active continental margin (the Palomares Margin, western Mediterranean). Geomorphology 219, 10–26. https://doi.org/10.1016/j.geomorph.2014.04.014.

Puig, P., Palanques, A., Sanchez-Cabeza, J.A., Masque, P., 1999. Heavy metals in particulate matter and sediments in the southern Barcelona sedimentation system (Northwestern Mediterranean). Mar. Chem. 63, 311–329. https://doi.org/10.1016/S0304-4203(98)00069-3.

Puig, P., Canals, M., Company, J.B., Martin, J., Amblas, D., Lastras, G., Palanques, A., Calafat, A.M., 2012. Ploughing the deep sea floor. Nature 489, 286–290. https://doi.org/10.1038/nature11410.

Puig, P., Palanques, A., Martín, J., 2014. Contemporary sediment-transport processes in submarine canyons. Annu. Rev. Mar. Sci. 6, 53–77. https://doi.org/10.1146/annurev-marine-010213-135037.

Puig, P., Durán, R., Muñoz, A., Elvira, E., Guillén, J., 2017. Submarine canyon-head morphologies and inferred sediment transport processes in the Alías-Almanzora canyon system (SW Mediterranean): On the role of the sediment supply. Mar. Geol. 393, 21–34. https://doi.org/10.1016/j.margeo.2017.02.009.

Pusceddu, A., Bianchelli, S., Martín, J., Puig, P., Palanques, A., Masqué, P., Danovaro, R., 2014. Chronic and intensive bottom trawling impairs deep-sea biodiversity and ecosystem functioning. Proc. Nat. Acad. Sc. 11 (24), 8861–8866. https://doi.org/10.1073/pnas.1405454111.

Radakovitch, O., Roussiez, V., Olliver, P., Ludwig, W., Grenz, C., Probst, J.-L., 2008. Input of particulate heavy metals from rivers and associated sedimentary deposits on the Gulf of Lion continental shelf. Estuar. Coast. Shelf Sci. 77, 285–295. https://doi.org/10.1016/j.ecss.2007.09.028.

Raiswell, R., 2011. Iron transport from the continents to the open ocean: the aging rejuvenation cycle. Elements 7, 101e106. https://doi.org/10.2113/gselements.7.2.101.

Richter, T.O., de Stigter, H.C., Boer, W., Jesus, C.C., van Weering, T.C.E., 2009. Dispersal of natural and anthropogenic lead through submarine canyons at the Portuguese margin. Deep. Res. Part I Oceanogr. Res. Pap. 56, 267–282. https://doi.org/10.1016/j.dsr.2008.09.006.

Ross, C.B., Gardner, W.D., Richardson, M.J., Asper, V.L., 2009. Currents and sediment transport in the Mississippi Canyon and effects of Hurricane Georges. Cont. Shelf Res. 29, 1384–1396. https://doi.org/10.1016/j.csr.2009.03.002.

Roussiez, V., Ludwig, W., Monaco, A., Probst, J.-L., Bouloubassi, I., Buscail, R., Saragoni, G., 2006. Sources and sinks of sediment-bound contaminants in the Gulf of Lions (NW Mediterranean sea): a multi-tracer approach. Cont. Shelf Res. 26, 1843–11857. https://doi.org/10.1016/j.csr.2006.04.010.

Roussiez, V., Heussner, S., Ludwig, W., Radakovitch, O., Durrieu de Madron, X., Guieu, C., Probst, J.L., Monaco, A., Delsaut, N., 2012. Impact of oceanic floods to particulate metal inputs to coastal and deep sea environments: a case study in the Northwest Mediterranean. Cont. Shelf Res. 45, 15–26. https://doi.org/10.1016/j.csr.2012.05.012.

Rudnick, R.L., Gao, S., 2003. In: Rudnick, R.L. (Ed.), Treatise of Geochemistry, 3. Elsevier, Amsterdam, pp. 1–64. https://doi.org/10.1016/B0-08-043751-6/03016-4.

Rumín-Caparrós, A., Sanchez-Vidal, A., González-Pola, C., Lastras, G., Calafat, A., Canals, M., 2016. Particle fluxes and their drivers in the Avilés submarine canyon and adjacent slope, central Cantabrian margin, Bay of Biscay. Progr. Oceanogr. 144, 39–61. https://doi.org/10.1016/j.pocean.2016.03.004.

Rusiecka, D., Gledhill, M., Milne, A., Achterberg, E.P., Annett, A.L., Atkinson, S., Birchill, A., Karstensen, J., Lohan, M., Mariez, C., Middag, R., Rolison, J.M., Tanhua, T., Ussher, S., Connelly, D., 2018. Anthropogenic signatures of lead in the Northeast Atlantic. Geophys. Res. Lett. 45 (6), 2734–2743. https://doi.org/10.1002/2017GL076825.

Sanchez-Vidal, A., Calafat, A., Canals, M., Fabres, J., 2004. Particle fluxes in the Almeria-Oran front: control by coastal upwelling and sea-surface circulation. J. Mar. Syst. 52, 89–106. https://doi.org/10.1016/j.jmarsys.2004.01.010.

Sanchez-Vidal, A., Collier, R.W., Calafat, A., Fabres, J., Canals, M., 2005. Particulate barium fluxes on the continental margin: a study from the Alboran Sea (Western Mediterranean). Mar. Chem. 93 (2–4), 105–117. https://doi.org/10.1016/j.marchem.2004.07.004.

Tarrés, M., Cerdà-Domènech, M., Pedrosa-Pàmies, R., Rumín-Caparrós, A., Calafat, A., Canals, M., Sanchez-Vidal, A., 2022. Particle fluxes in submarine canyons along a sediment-starved continental margin and in the adjacent open slope and basin in the SW Mediterranean Sea. Prog. Oceanogr. 203, 102783 https://doi.org/10.1016/j.pocean.2022.102783.

Tebo, B.M., Bargar, J.R., Clement, B.G., Dick, G.J., Murray, K.J., Parker, D., Verity, R., Webb, S.M., 2004. Biogenic manganese oxides: Properties and mechanisms of formation. Annu. Rev. Earth Planet. Sci. 32 (1954), 287–328. https://doi.org/10.1146/annurev.earth.32.101802.120213.

Tesi, T., Puig, P., Palanques, A., Goñi, M.A., 2010. Lateral advection of organic matter in cascading-dominated submarine canyons. Prog. Oceanogr. 84 (3–4), 185–203. https://doi.org/10.1016/j.pocean.2009.10.004.

Theodosi, C., Parinos, C., Gogou, A., Kokotos, A., Stavrakakis, S., Lykousis, V., Hatzianestis, J., Mihalopoulos, N., 2013. Downward fluxes of elemental carbon, metals and polycyclic aromatic hydrocarbons in settling particles from the deep Ionian Sea (NESTOR site), Eastern Mediterranean. Biogeosciences 10, 4449–4464. https://doi.org/10.5194/bg-10-4449-2013.

Thibault de Chanvalon, A., Metzger, E., Mouret, A., Knoery, J., Chiffoleau, J.F., Brach-Papa, C., 2016. Particles transformation in estuaries: Fe, Mn and REE signatures through the Loire Estuary. J. Sea Res. 118, 103e112. https://doi.org/10.1016/j.seares.2016.11.004.

Tintore, J., La Violette, P.E., Blade, I., Cruzado, A., 1988. A study of an intense density front in the Eastern Alboran Sea: the Almeria-Oran Front. J. Phys. Oceanogr. 18, 1384–1397. https://doi.org/10.1175/1520-0485(1988)018<1384:ASOAID>2.0.CO;2.

Twining, B.S., Baines, S.B., 2013. The trace metal composition of marine phytoplankton. Annu. Rev. Mar. Sci. 5 (1), 191–215. https://doi.org/10.1146/annurev-marine-121211-172322.

Vargas-Yáñez, M., Plaza, F., García-Lafuente, J., Sarhan, T., Vargas, J.M., Vélez-Belchi, P., 2002. About the seasonal variability of the Alboran Sea circulation. J. Mar. Syst. 35 (3–4), 229–248. https://doi.org/10.1016/S0924-7963(02)00128-8.

Yiğiterhan, O., Murray, J.W., Tuğrul, S., 2011. Trace metal composition of suspended particulate matter in the water column of the Black Sea. Mar. Chem. 126, 207–228. https://doi.org/10.1016/j.marchem.2011.05.006.